1 NAME, SURNAME

Anna Makal

2 HELD DIPLOMAS, SCIENTIFIC DEGREES

24 February 2010 Doctor of Philosophy degree in chemistry obtained at the Chemistry Department, Warsaw University, Supervisor: prof. dr hab. K. Woźniak; Thesis: 'The structural and charge density analysis of selected iron and ruthenium compounds in the solid state'.

21 June 2004 Master degree in chemistry obtained at Laboratory of Crystallography, Chemistry Department, Warsaw University, Supervisor: prof. dr hab. K. Woźniak; Thesis: 'Structure determination and refinement of the human dihydrolipoamide dehydrogenase (E3) enzyme complexed with its binding protein (E3BP)'

29 September 2003 Bachelor degree in molecular biology obtained at Institute of Microbiology, Biology Department, Warsaw University, Supervisor: prof.dr hab. K.Jagusztyn-Krynicka Thesis: 'Zastosowanie metod krystalograficznych w badaniach oddziaływań białko-białko – analiza struktury białka opiekuńczego SecB', in english: 'Application of crystallography in analysis of protein-protein interactions – the structure of chaperon protein SecB'

3 CURRENT AND PREVIOUS EMPLOYMENT

in research institutions

1 October 2013 – present Adjunct,
Warsaw University, Department of Chemistry, Warsaw, Poland
Structural and charge density oriented crystallography. Investigating relationships between structure and photoactivity in the solid state.

28 January 2013 – 30 September 2013 Crystallographer (Technician),
Warsaw University, Department of Chemistry, Warsaw, Poland
Structural and charge density oriented crystallography.

1 July 2010 – 20 October 2012 Research Scholar,
SUNY at Buffalo, Department of Chemistry, Buffalo, NY, USA
Methodology and applications of Laue photocrystallography on organometallic complexes.

1 March – 1 June 2010 Crystallographer (Technician),
Warsaw University, Department of Chemistry, Warsaw, Poland
Structural and charge density oriented crystallography.

10 July – 29 August 2005 Research Scholar,
Department of Molecular Physiology and Biological Physics, University of Virginia, Charlottesville VA, USA
Experimental charge density analysis,

9 February – 15 September 2003 Research Scholar,
Marshall Space Flight Center, Huntsville, AL, USA
Protein crystallography on human pyruvate dehydrogenase.

4 INDICATION OF ACHIEVEMENT

4.1 TITLE

Estimation of the impact of crystalline environment on the physicochemical properties of materials using non-standard crystallographic techniques

4.2 PUBLICATIONS comprising the academic achievement

[H1] Jason B. Benedict, **Anna Makal**, Jesse D. Sokolow, Elzbieta Trzop, Stephan Scheins, Robert Henning, Timothy Graber, and Philip Coppens*.
Time-resolved Laue diffraction of excited species at atomic resolution: 100 ps single-pulse diffraction of the excited state of the organometallic complex $Rh_2(\mu\text{-}PNP)_2(PNP)_2{\cdot}BPh_4$.
Chemical Communications, 47(6):1704–1706, January 2011.
IF = 6.1, citations 55
My contribution: participation in the experimental data collection and data processing, testing several models of excited state and several refinement procedures, proposing a new method of calculating the type-II photodifference-map, proposing a new method of scaling and combining data from several experiments, selecting the final model of the excited state, writing a part of the manuscript. About 30%

[H2] **Anna Makal**, Elżbieta Trzop, Jesse Sokolow, Jarosław Kalinowski, Jason Benedict, and Philip Coppens*.
The development of Laue techniques for single-pulse diffraction of chemical complexes: time-resolved Laue diffraction on a binuclear rhodium metal-organic complex.
Acta Crystallographica Section A: Foundations of Crystallography, 67(4):319–326, July 2011.
IF = 4.2, citations 26
My contribution: participation in the experimental data collection data and data processing, testing several models of excited state and several refinement procedures, proposing a new method of calculating the type-II photodifference-map, selecting the final model of the excited state, writing a part of the manuscript. About 40%

[H3] Jarosław A. Kalinowski*, **Anna Makal**, and Philip Coppens.
The LaueUtil toolkit for Laue photocrystallography. I. Rapid orientation matrix determination for intermediate-size-unit-cell Laue data.
Journal of Applied Crystallography, 44(6):1182–1189, December 2011.
IF = 4.3, citations 9
My contribution: providing experimental data, inspiring a new idea for the indexing method, testing and critically evaluating implemented indexing methods, writing a part of the manuscript. About 40%

[H4] Jarosław A. Kalinowski*, Bertrand Fournier, **Anna Makal***, and Philip Coppens.
The LaueUtil toolkit for Laue photocrystallography. II. Spot finding and integration.
Journal of Synchrotron Radiation, 19(4):637–646, July 2012.

IF = 3.0, citations 8
My contribution: providing experimental data, testing and critically evaluating several methods of data processing, proposing improved tests for new algorithms, writing a part of the manuscript. About 30%

[H5] **Anna Makal**, Jason Benedict, Elzbieta Trzop, Jesse Sokolow, Bertrand Fournier, Yang Chen, Jarosław A. Kalinowski, Tim Graber, Robert Henning, and Philip Coppens*.
Restricted Photochemistry in the Molecular Solid State: Structural Changes on Photoexcitation of Cu(I) Phenanthroline Metal-to-Ligand Charge Transfer (MLCT) Complexes by Time-Resolved Diffraction.
The Journal of Physical Chemistry A, 116(13):3359–3365, April 2012.
IF = 2.6, citations 8
My contribution: participation in the experimental data collection and data processing using newly-designed methods, testing several excited state models and a number of refinement procedures, finding the final excited state model for two independent molecules of the tested compound, writing a part of the manuscript. About 45%

[H6] Philip Coppens*, Jesse Sokolow, Elzbieta Trzop, **Anna Makal**, and Yang Chen.
On the Biexponential Decay of the Photoluminescence of the Two Crystallographically-Independent Molecules in Crystals of $[Cu(I)(phen)(PPh_3)_2][BF_4]$.
The Journal of Physical Chemistry Letters, 4(4):579–582, February 2013.
IF = 8.5, citations 18
My contribution: participation in the experimental data collection and data processing, testing several excited state models and several refinement procedures, proposing a new method of scaling and combining data from several experiments, finding the final excited state model for two independent molecules of the tested compound, writing a part of the manuscript. About 30%

[H7] Daniel Tchoń, and **Anna Makal***.
Structure and piezochromism of pyrene-1-aldehyde at high pressure.
Acta Crystallographica Section B: Structural Science, Crystal Engineering and Materials, Accepted, March 2019.
IF = 4.2, citations 0
My contribution: design of the research project, participation in the experimental data collection and data processing, interpretation of the results, writing a final version of the manuscript. About 55%

[H8] **Anna Makal***, Joanna Krzeszczakowska, and Roman Gajda
Pressure-Dependent Structural and Luminescence Properties of 1-(pyren-1-yl)but-2-yn-1-one.
Molecules, 24, 1107; doi:10.3390/molecules24061107, March 2019.
IF = 3.2, citations 0
My contribution: design of the research project, participation in the experimental data collection, data processing, theoretical calculations, interpretation of the results, writing a final version of the manuscript. About 75%

[H9] Roman Gajda, Mateusz A. Domański, Maura Malinska, and **Anna Makal***.
Crystal morphology fixed by interplay of pi-stacking and hydrogen bonds – the case of 1-hydroxypyrene.
CrystEngComm, 21:1701–1717, March 2019.
IF = 3.2, citations 0
My contribution: design of the research project, participation in the experimental data collection and data processing, interpretation of the results, writing a final version of the manuscript. About 60%

[H10] **Anna Makal***.
Triethylphosphine as a molecular gear – phase transitions in ferrocenyl–acetylide–gold(I).
Acta Crystallographica Section B: Structural Science, Crystal Engineering and Materials, 74(5):427–435, October 2018.
IF = 4.2, citations 0
My contribution: This work was performed by myself. 100%

Impact factor and citations according to the Web of Science as of January 30-th 2019
* – corresponding author

4.3 DISCUSSION OF THE SCIENTIFIC GOALS of the above publications and the results achieved together with a discussion of their possible use

4.3.1 Introduction

X-ray crystallography from the very beginning has been a very important technique for chemistry. From the crystal structure of diamond [1], through ending a long ambiguity concerning the true structure of ferrocene [2, 3, 4] and determination of the more complex structures of vitamins [5] and proteins [6, 7], or confirmation of the true enantiomer of chiral substances [8] it has been extremely useful in confirming many chemical hypotheses. It is a key technique to establish the exact conformation of the analyzed molecule in crystal. Nowadays it can, however, go well beyond determination of atomic positions and bond lengths, averaged over time and a crystal bulk.

Experimental charge density analysis gives insight into charge distribution and into the character of chemical bonds, sometimes re-defining them and linking experiment to quantum-chemical theories (QTAIM) and concepts.

Studying rearrangements occurring in the crystal structures under pressure can be the means of ascertaining the importance and relative hierarchy of intermolecular interactions [61, 59, 60].

Analysis of diffuse X-ray scattering allows to characterize local departures from an average crystal structure, so called 'local order', the existence of which usually connected with such important physical properties of materials as ferromagnetism [9] or ferroelectricity [10].

Finally, photocrystallographic techniques go beyond static structure determination toward investigation of dynamic processes. They allow to track chemical reactions in the solid state and to determine structures of molecules in excited state, as short lived as a few nanoseconds [11].

In my scientific career before obtaining PhD I was privileged enough to participate in studies representing many of the above crystallographic challenges, from determination of the structure of a protein complex [B5], through structural analysis of a number of organic (e.g. [B11, B13]), metalorganic (e.g. [B12, B17]) and inorganic (e.g. [B10]) compounds to experimental charge density analysis involving characterization of both intra- and intermolecular interactions [B6, A2, A3].

The collection of scientific publications which I present here also comprises a few aspects of modern applied crystallography, including photocrystallography, high-pressure crystallography and tracing the mechanism of Single-Crystal-to-Single-Crystal (SCSC) phase transitions.

There are three aspects that these studies have in common:

- they all reach beyond characterization of molecular structure in the crystal; in fact, their results represent the importance of considering the crystalline environment and its impact on the properties of molecular species within a bulk,
- they all aim at explaining macroscopic physicochemical properties of analyzed materials on the basis of crystal structure and resulting electronic properties,
- in a way they all involved experiments at non-ambient conditions: either under excitation by UV light, at very high pressure or in the vicinity of phase transitions and required application of non-standard methods.

4.3.2 Ultra-fast photocrystallography using Laue diffraction techniques

Photocrystallography was probably best defined by the late prof. Philip Coppens as a science which 'combines X-ray diffraction with external light excitation of the sample; it is utilized for studying out-of-equilibrium phenomena in crystals, i.e. relaxation processes, long-lived metastable states, short-lived excited states or solid-state photochemical reactions' (from the Introduction to Workshop on Dynamic Structural Photocrystallography in Chemistry & Materials Science at Buffalo, NY, USA, June 2013)

As such, it covers a wide range of physicochemical processes which occur on many different time-scales, ranging from photochemical reactions which can take hours to light-induced electron excitations, where excited states display lifetimes in microsecond or nanosecond regime. The term "Time-resolved" (TR) X-ray crystallography can be applied in the latter case. TR photocrystallography finds applications in photovoltaics, optoelectronics, biosensors and general design of functional materials by tracking:

- propagation of changes in a bulk (e.g. appearance and displacement of defects, uncovering mechanisms and propagation of phase transitions),
- changes in molecular structures resulting from electronic excitations in photosensitizer dyes or optoelectronic components,
- photomagnetic effects (molecular memory designing),
- mechanisms of biochemical processes.

At the same time, observation of short-lived excited-state species or very fast transformations in the solid state poses several challenges:

- the transformation should be induced in as large a part of the crystalline sample, as possible; this requires for instance access to a strong light source (laser) - a 'pump' - for photoexcitation,
- the X-ray radiation (probe) must be timed to the factor triggering observed change (e.g. a light pulse) in order to probe the structure before the excited state relaxes or the transformation process completes,
- at the same time, X-ray radiation must be powerful enough for diffraction from a small or only partially excited / transformed sample to be observable,
- there is a significant risk of sample deterioration under the intense 'pump' and 'probe' radiation, so the experiments must be adjusted for maximum speed and efficiency.

It follows, that TR crystallography requires dedicated equipment including the change-initiating 'pump' sources (e.g. powerful lasers), the state-of-the-art X-ray 'probe' sources and the fast X-ray detection tools. Often it can only be performed at dedicated synchrotron stations which offer ultra-bright, ultra-short pulses of X-ray radiation. The experiments are in each research case quite unique and require many test attempts to determine optimal conditions and protocols. Last but not least, experimental data acquired at highly non-standard conditions require new ways of processing, and quite often a dedicated software.

A comprehensive summary on the state of photocrystallography in year 2017 has been published by Coppens [11], in whose group the methods for ultra-fast photocrystallography have been developed for years.

Back in 2010, at the beginning of my post-doctoral stay at prof. Coppens, there were known examples of TR studies in which atomic resolution was reached and a reasonable accuracy achieved with monochromatic X-ray radiation [12, 13]. However, only a very small fraction of the photons in the synchrotron beam could be productively used with monochromatic radiation. As a result, longer exposure times and therefore more pulses were required, which limited the time resolution that could be achieved. Furthermore, longer exposure time implied more extensive pump laser exposure, increasing the temperature of a crystal due to light absorption and the risk of sample deterioration due to heating and radiation damage.

For prof. Coppens it followed that for sub-microsecond-timescale TR diffraction at synchrotron sources the use of polychromatic radiation was necessary (Laue technique). It would enable one to use the X-ray beam more efficiently, as more diffraction signals could be registered when multiple wavelength radiation was used all at once, and lack of monochromatization would result in an X-ray beam a few orders of magnitude stronger, leading to a shorter experiment time and reducing the risk of sample deterioration.

On the other hand, new methods had to be developed to handle all the problems posed by the wavelength dependence of the diffracted intensities and the detector response. A few such methods originated in the prof. Coppens group, including:

- the RATIO technique [14] in which the Ratios R of measured X-ray intensities $\mathrm{I}^{ON}/\mathrm{I}^{OFF}$ are used in combination with a set of monochromatic data collected at the same temperature ($\mathrm{I}^{ON}/\mathrm{I}^{OFF}$ denoting diffracted X-ray intensities collected when the 'pump' has been activated or not, accordingly). The I^{ON} are obtained by multiplication of the monochromatic diffraction intensities by the synchrotron-determined Ratios R
$$I^{ON} = I_{monochromatic} R.$$
In some considerations, response ratios η
$$\eta = R - 1$$
are more convenient to use;
- the definition of R-factors specific for dynamic structure crystallography [15],
- dedicated LASER2010 software to use the RATIO method in structure refinement [16],
- photo-Wilson plots to estimate the temperature increase due to the laser exposure of the sample [11],
- an approach to retrieve multi-wavelength X-ray diffracted intensities using seed-skewness method [12, 17].

The challenges which still remained when I joined prof. Coppens group in year 2010 included:

- the lack of effective method for X-ray diffraction data indexing; available algorithms and software were optimized for protein samples, in which a single diffraction image contained on average 10 to 100 times more reflections,

- the need for a quick and efficient method to retrieve diffracted intensities in order to assess, whether the sample is indeed responding to the excitation source,
- the fact that tested samples were still prone to deteriorate before a relatively complete data set could be collected and necessity to handle numerous incomplete data sets.

Last but not least, proper choice of the investigated crystalline material had to be made. A number of publications from prof. Coppens group at that time revolved around the ways, in which supramolecular environment influenced the activity of selected luminophores [18, 19], sometimes quenching their luminescence [20].

Excited state of metalorganic complex isolated in the crystal lattice

The aim of the studies described in [H1] and [H2] was to conduct time-resolved atomic-resolution crystallographic analysis using Laue technique at the synchrotron source and to obtain improved accuracy as compared with previous monochromatic photocrystallographic studies.

The investigated compound (RhPNP) was $Rh_2(\mu\text{-PNP})_2(PNP)_2{\cdot}BPh_4$, where PNP = $CH_3N(P(OCH_3)_2)_2$ and Ph = phenyl (Figure 1a). Its choice was dictated by several factors. Firstly, it was similar to compounds on which successful photocrystallographic studies were performed using monochromatic X-ray sources [21, 22]. Secondly, the photochemistry of this compound and related salts was already studied in detail by Mague and coworkers [23, 24], and excited state lifetimes were known to be in μs regime at liquid nitrogen temperatures. Thirdly, crystal structure of the α-polymorph of RhPNP ensured, that each photon-absorbing cation in the crystal structure is separated from the other cations, being enclosed in the phenyl arms of the BPh_4 anions (Figure 1). Structural changes in RhPNP cation induced by photoexcitation would not therefore produce strain in the crystal structure and did not result in unit cell changes upon excitation. It allowed to assume a 'random' model of occurrence of excitations in the crystal [25].

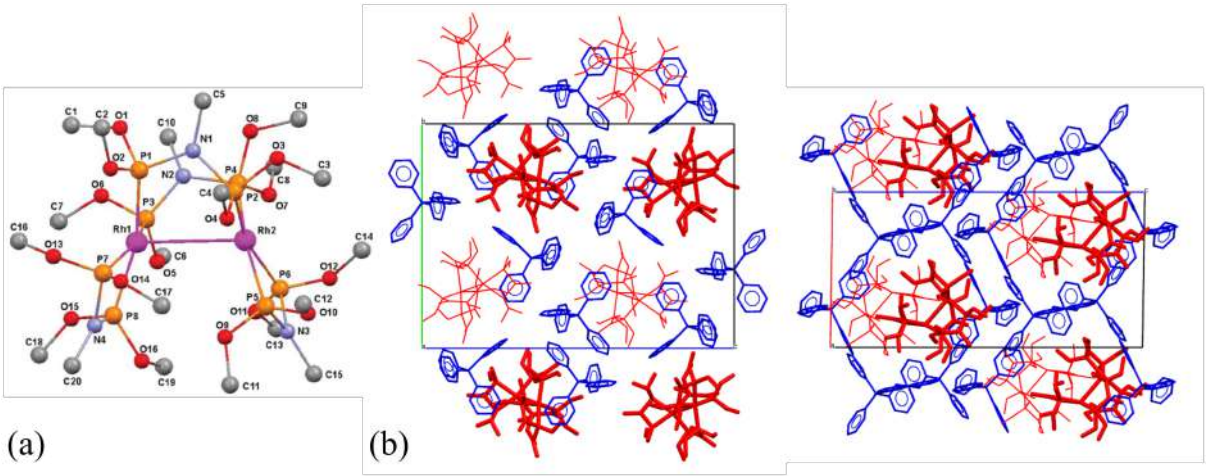

Figure 1: (a) The schematic view of the RhPNP cation; H-atoms omitted for clarity (Fig. 1 in [H2]) and (b) the RhPNP cations (red) enclosed between the BPh_4 anions (blue), view of the crystal structure in [100] direction (left) and in [101] (right).

Carefully planned experiments were described in detail in [H2]. The most important innovation with respect to former attempts at Laue photocrystallography was repeating

the OFF/ON pump-probe cycle 10 times for each crystal orientation. Repeated measurements allowed to estimate standard uncertainties of the obtained Ratios R, give more meaning to the correlations between data collected from several crystals, and sort out some spectacularly strong 'response ratios' which were in fact artifacts. A total of 6 datasets of sufficient quality were retained and combined together.

The excited-state populations according to the final structural model ranged from 4.7% to 6.6% depending on the crystal sample. The most prominent structural changes upon excitation involved the vicinity of Rh cations: a Rh–Rh distance contraction of 0.154(13) Å and a rotation of the Rh–Rh bond axis in the crystal (Figure 2) with respect to the ground state structure.

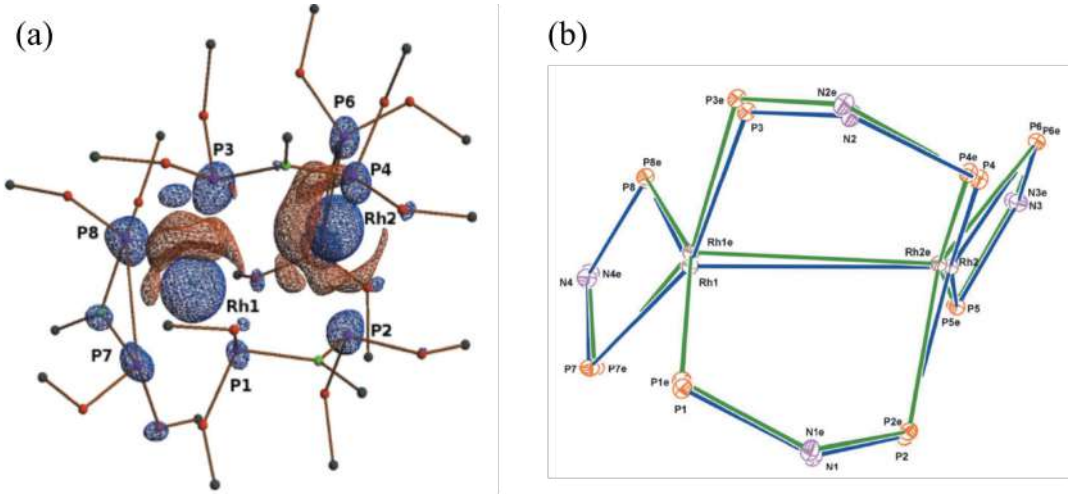

Figure 2: The structural changes occurring in the structure of RhPNP upon excitation: (a) type-II photodifference map for RhPNP with isosurfaces (red - positive, blue - negative) of +/-0.25 eÅ^{-3} (mesh) (Fig. 6 in [H2]) (b) the overlaid structures of the ground (blue lines) state and excited (green lines) state, the excited-state atoms are marked with 'e' after the label. Ellipsoids are drawn at the 5% probability level for the sake of clarity. (Fig. 7 in [H2])

The experimental contraction of the Rh–Rh bond in this Rh(I) complex was considerably less than observed in the former time-resolved studies of Rh complexes [21]. It was however in quantitative agreement with the results of theoretical calculations, once the presence of the crystalline environment was taken into account in the theoretical computations, by means of QMMM approach [26] (i.e. the closest neighborhood of the molecule for which quantum calculations were to be performed was reconstructed around it and treated with molecular mechanic methods: allowed to slightly adjust positions). It showed, that influence of the crystalline environment could not be neglected even in the case, where its only role was purely 'mechanic', i.e. just restricting the position of the excited state species and the volume available for it in the crystal structure.

The works [H1, H2] showed for the first time, that the improved Laue technique could be used for the determination of the structures molecular excited states at atomic resolution in crystals. Experimental standard deviation on metal–metal distance was 4 times smaller than those in previous monochromatic studies [21], while the experiments were completed in a much shorter time span, and with better time resolution.

My contribution to these works consisted of participation in the synchrotron data collection and data processing, testing several models of excited state and a number of refinement procedures and proposing the final model of the excited state of the analyzed compound. On the way, I proposed a method of scaling and combining data from several

incomplete experiments and a new approach to calculate photodifference Fourier maps, both explained in more detail below.

Methodology - data scaling

As already mentioned, describing structure of RhPNP in the excited state required combining 6 incomplete diffraction data sets, collected from 6 distinct crystals. A dedicated scaling procedure was necessary to accomplish it and to calculate so called 'photodifference maps' using all available reflections. In the course of my research presented in [H1, H2, H5, H6] I proposed and used the scaling method described below.

Data sets coming from distinct crystal samples were expected to show different populations of excited molecules and different extent of temperature-induced changes. To bring them to a common scale the η values of individual reflections were scaled by $\langle|\eta|\rangle_{set}/\langle|\eta|\rangle_{all}$, in which $\langle|\eta|\rangle_{all}$ and $\langle|\eta|\rangle_{set}$ were the averages over all measured reflections and over the reflections in the specific data set respectively.

Corrected ratio/response ratio values were obtained as:

$$k(\eta_{set}) = \langle|\eta|\rangle_{all} \,/\, \langle|\eta|\rangle_{set}$$

$$\eta_{scaled}(\mathbf{h}) = \eta(\mathbf{h})k(\eta)_{set}$$

$$R_{scaled}(\mathbf{h}) = 1 + \eta_{scaled}(\mathbf{h})$$

The scaled and merged ratios could then be used to generate uniform I^{ON} values for the calculation of photo-difference maps. The idea was later developed into a more sophisticated approach by Betrand Fournier [27, 28].

Possible temperature differences were taken into account independently in the LASER2010 program by introduction of a overall temperature-scale-factor k_B which multiplies the experimental atomic displacement parameters (ADP's) [11]. However, in these particular studies with Laue method temperature increases were moderate and k_B values did not exceed 1.3 (i.e. 30% increase in the average isotropic atomic temperature factor B).

Methodology - Photodifference Maps

A difference or residual Fourier map illustrates the differences between electron density predicted by the crystallographic model and the electron density resulting from experimental structure factors, with phases taken from the model.

$$\rho_0(\mathbf{r}) = \frac{1}{V}\sum_{\mathbf{h}}(F_{\text{obs}} - F_{\text{calc}})e^{i\varphi_{\text{calc}}}e^{-2\pi i\mathbf{hr}}$$

As phases φ in such calculations are common for both compared sets of structure factors, the differences are contained in the amplitudes $(F_{\text{obs}} - F_{\text{calc}})$. In the context of photocrystallography, a similar map may be devised, displaying the difference between the ground state (GS) and excited state (ES) structures.

$$\rho_0(\mathbf{r}) = \frac{1}{V}\sum_{\mathbf{h}}(F_{\text{obs}}^{ON} - F_{\text{obs}}^{OFF})e^{i\varphi_{\text{calc}}^{OFF}}e^{-2\pi i\mathbf{hr}}$$

This photo-difference map would be denoted as photo-difference type-I map. In Laue diffraction experiments and with data processing concentrated on retrieving experimental Ratios R, photodifference type-I map coefficients would have to include X-ray amplitudes and phases from a reference monochromatic experiment (REF):

$$\rho_0(\mathbf{r}) = \frac{1}{V}\sum_{\mathbf{h}}(F_{\text{obs}}^{ON} - F_{\text{obs}}^{REF})e^{i\varphi_{\text{calc}}^{REF}}e^{-2\pi i\mathbf{hr}}$$

As such it could contain discrepancies arising for instance from subtle differences in unit cell parameters of the reference structure and the excited state structure or from inconsistencies in measurement temperatures registered on different setups. The effect of excitation could in fact be masked by the above mentioned effects.

Photo-difference type-II map on the other hand was proposed by me to exclude all features which might arise from the difference between the data from reference crystal and the data from the crystal actually subjected to the experiments at the synchrotron. Its calculation requires, that a map with

$$(F_{\text{obs}}^{OFF} - F_{\text{obs}}^{REF})$$

coefficient is also computed, and than subtracted from the type-I photodifference map.

The resulting map calculated for RhPNP showed distinct features indicating the structural transformation in the excited state (Figure 2a).

Methodology - Fast Laue X-ray Data Indexing

Indexing of the X-ray diffraction pattern means that each diffracted signal is assigned to a set of lattice planes on which the diffraction took place. Each family of planes is identified by a unique vector $\mathbf{h}$, normal to these planes, and a full collection of such normal vectors can be represented as a reciprocal lattice for a given crystal.

With a polychromatic X-ray beam most of the reciprocal-lattice points within the resolution limits $1/d_{\text{res}}$ and between the limiting Ewald spheres of radii $1/\lambda_{\text{min}}$ and $1/\lambda_{\text{max}}$ can in principle be recorded on a single image, and in practice on a few images. The Bragg diffraction condition can be written as:

$$\mathbf{h}_i = \frac{1}{\lambda_i}(\mathbf{s}_i - \mathbf{s}^0)$$

where $\mathbf{s}^0$ and $\mathbf{s}_i$ are dimensionless unit vectors with directions aligned with the primary and diffracted X-ray beams respectively for spot i and λ_i is the wavelength at which the spot was recorded. Both unit vectors and the Bragg angle θ_i can be calculated from the experimental data, i.e. from the positions of the diffracted signals on a detector and from the geometry of the goniometer and detector placement (Section 2.1 in [H3]).

When the unit cell of the investigated crystal is known, for instance from the reference monochromatic experiment, the indexing problem is reduced to finding the orientation of this unit cell with respect to the goniometer reference system.

In monochromatic diffraction studies where the wavelength λ_i is known, this step is usually straightforward. Moreover, indexing is used to distinguish between the sample diffraction data and artifacts resulting for instance from icing, impurities or bad pixels prior to estimation of diffracted intensities.

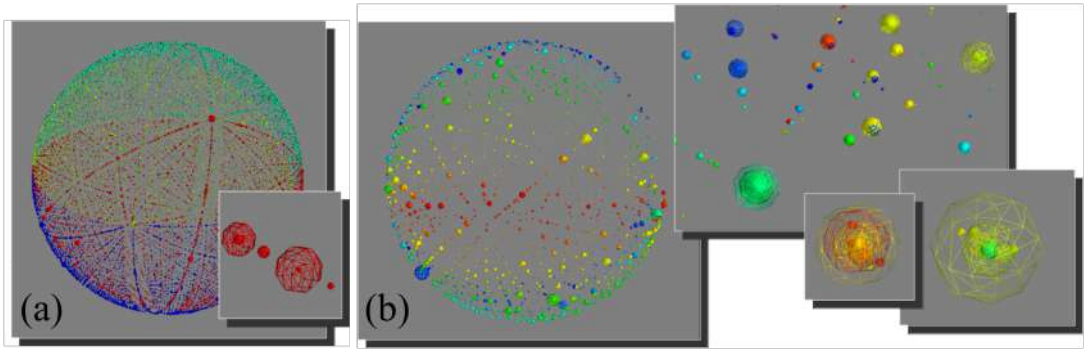

Figure 3: Representation of the reciprocal lattice vectors $\mathbf{h}_i$ projected on a sphere: (a) a reference, complete data set, color-coded by symmetry equivalence; clusters of reflections are well defined, with points all in the center of the cluster (inset); (b) the projection of a data set from Laue experiment; reflections are clustered 'around' a central point, not exactly in it, due to experimental errors. Wireframe sphere sizes proportional to diffracted intensities.

However, in the case of X-ray Laue diffraction it is impossible to determine λ_i by experimental means, as detectors lack the ability of discrimination between photons of different energy (wavelength). The length of $\mathbf{h}_i$ can not be determined either and derivation of the exact cell parameters and the unit cell volume requires additional information.

In order to apply geometrical algorithms a projection of $\mathbf{h}_i$ vectors onto a unit sphere was used:

$$\hat{\mathbf{h}}_i := \frac{\mathbf{h}_i}{|\mathbf{h}_i|}.$$

When the coordinates of the observed peaks are transformed to the goniometer-head coordinate system all registrations from different frames having the same *hkl* indices (i.e. representing diffraction from the same family of lattice planes), recorded at different λ should project exactly at the same point on the unit sphere. The same point on the unit sphere should also be shared by the other reciprocal lattice points located on the same ray (e.g. reflections with (111), (222) and (333) indices). In practice, due to errors in the peak-center determination, the experimentally determined $\hat{\mathbf{h}}$ vectors for a given *hkl* will form a cluster of points on the sphere located around the ideal position (Figure 3).

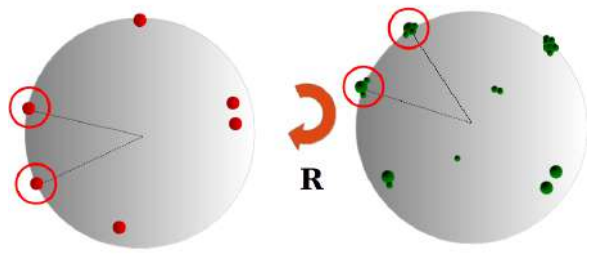

Figure 4: The schematic representation of the problem of finding orientation matrix R - the rotation resulting in the most effective overlay of two patterns on the sphere. Reference data represented in red (hkl indices for each spot are known), the Laue experiment results - in green.

In addition, spurious signals not resulting from Bragg diffraction (cosmic radiation, bad pixels and artifacts generated by the spot-finding algorithm) will project as randomly distributed isolated points on the sphere. In the first approximation, any signal not within a cluster can be excluded from the initial indexing procedure.

The problem of finding an orientation matrix can then be reduced to the problem of finding the most efficient overlay of the experimental pattern of clusters projected on a unit sphere centered on the origin of the reciprocal lattice with the corresponding pattern from a monochromatic data set (reference data set) of the same material (Figure 4). Once an effective overlay has

been obtained and orientation matrix determined, specific indices and wavelengths can be assigned to each diffraction spot.

The technique is applied to the complete reference data set and eliminates problems encountered when few frames with a limited number of peaks are to be used for orientation matrix determination (as is the case with deteriorating samples in photocrystallography or very short preliminary experiments). As it uses patterns projected on a sphere, it is not only wavelength-independent, but also robust with respect to small discrepancies between the temperature of the Laue experiment and the reference experiment - an important point, as the monochromatic data are never collected in exactly the same conditions as the Laue data).

The work [H3] details the derivation for this method, describes the implementation in a LaueUtil package and the results of testing it on a series of Laue X-ray diffraction data sets from organometallic crystals. The new indexing procedure yielded the averaged orientation matrix giving the best fit to the collected frames in all test instances, suitable for direct data integration of the data. Completeness of obtained data was very close to one achievable with frame-to-frame refined cell parameters and orientation matrices, with a gain in the number of data sets it could be applied to, data processing time and the ease of use. The method was successfully used in a few photocrystallographic studies [H5, H6] [29, 30]. My particular contribution to this work was inspiring the idea of using the projection on the unit sphere to circumvent the lack of information about the X-ray wavelength and extensive testing of the method while it was being developed.

Methodology - Fast and Efficient Integration of Laue X-ray Intensities

A new approach to Laue X-ray data integration from CCD was proposed in [H4], using simple statistical tools for identification of the background values for a given pixel on all frames in a scan, and identifying a Bragg diffraction signal as an outlier in background, independent from an indexing procedure. Two particular approaches were described, their applicability depending on the X-ray measurement strategy.

The major assumption of the method was that when a series of diffraction images is registered on a CCD detector from crystalline sample at several orientations, the majority of the signals on any given pixel contain just a background noise. Registration of the Bragg signal will be a rare-event, and such signal will be an outlier in a background distribution. The second important assumption was that the background noise did not change for the duration of the experiment.

For each of the pixels, intensity values were collected from all frames, leading to one-dimensional arrays which were statistically analyzed to estimate the background contributions for each of the individual pixels. The idea is illustrated in Figure 5a.

The estimate of the background on the frames was achieved by identifying and excluding outliers in per-pixel samples. The simplest approach ('constant fraction approach') was to assume that a certain percentage (usually about 20%) of the highest values along a pixel line (i.e. all values of a specified pixel on the successive frames) represent contributions from Bragg diffraction (Figure 5b). Remaining values were used to estimate the parameters of background distribution for each pixel.

For a photocrystallographic pump-probe experiment with a series of repeated measurements made both with or without the laser pump-pulses (ON and OFF frames) at each crystal orientation (e.g. 10), additional statistical tools could be used for background estimation [31, 32].

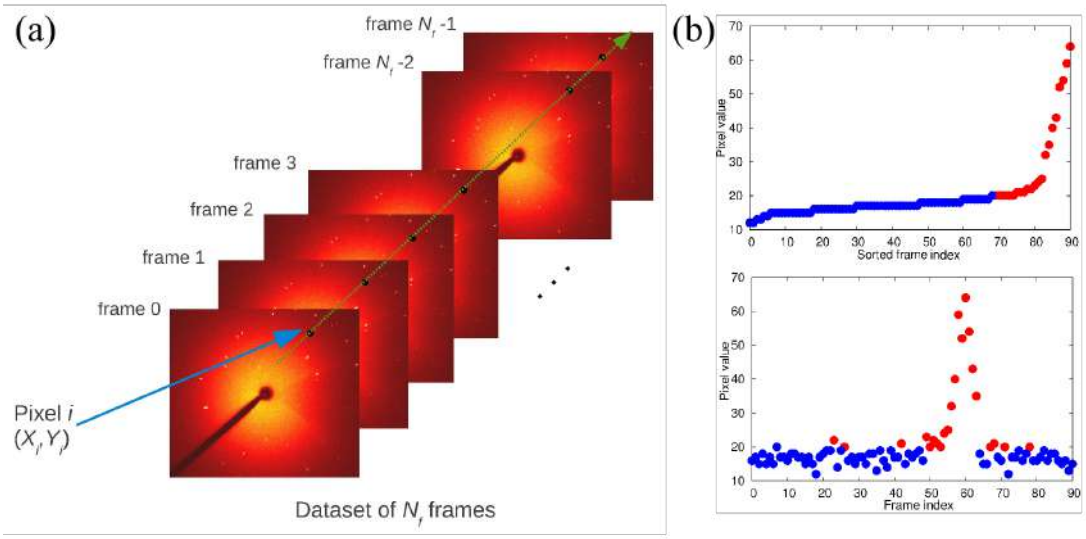

Figure 5: (a) Construction of a statistical sample of values for a chosen pixel: the values for a given pixel are collected for all frames in chronological order; (b) Example of statistical analysis performed using the constant-fraction method on the pixel (657,1014) of dataset 2. (top) sorted pixel values; (bottom) a plot of pixel values as a function of frame indices in the dataset. Blue dots correspond to background contributions, and red dots – to outliers (Fig. 1 and 2 in [H4])

The next processing step consisted of defining the mask which separated reflections from the background, and optimizing it. Diffraction spots have a non-negligible size and some definite shape, hardly ever as simple as circular or elliptical in photocrystallographic experiments. To retrieve reflection shapes, binary morphological operations [33] were applied: erosion operations removed isolated pixels or lines from a mask; then, dilation operations were used to add back some relevant pixels lost during erosion operations (Figure 4 in [H4]).

Finally, the processed masks were analyzed to determine the footprints of each of the reflections which were subsequently integrated to obtain the corresponding intensities and response ratios. The procedure described above was carried out on a pixel-by-pixel basis and was completely insensitive to the spatial relationships of the pixels.

The major advantage of the method was its being strictly based on statistical analysis of the pixel values, completely independent from any data indexing routine. It therefore allowed to monitor X-ray intensities and light-induced changes even when cell parameters were unknown, or indexing was complicated by crystal splitting or twinning (i.e. simultaneous diffraction from multiple crystal lattices).

In the case of ultra-fast photocrystallographic experiments the response ratios could be promptly obtained, analyzed (plotted or otherwise processed) to ascertain whether or not there were systematic ON versus OFF differences, and the experimental conditions could be adjusted accordingly.

In its current implementation the presented method was applicable mainly to data from photocrystallographic synchrotron experiments [H5, H6] [29, 30], although conventional data could also be processed with the constant-fraction approach.

My major role in this project was discussing the effects which usually determine the background distribution in an X-ray experiment with the code developers and then devising and conducting a series of tests, in which the results of the proposed method were compared with the intensities obtained from established software LaueGUI [17, 12]. The default parameter values in this method were the results of this extensive testing.

One chemical species - two types of response

Cu(I)[(1,10-phenanthro-line-N,N')-bis(triphenylphosphine)] is a model metalorganic complex which undergoes Metal-Ligand Charge Transfer (MLCT) as a result of electronic excitation by means of UV light. The MLCT means that in the excited state electron in this complex is transferred from the metal center to the organic ligand. If organic part of such a complex were chemically connected to a semiconductor with properly selected band structure (i.e. if the energy of the excited state resulting in MLCT is close to the level of conduction band of the substrate), the electron on the ligand could then get transferred into the conduction band of the substrate and initiate current flow. This is a process underlying photovoltaics: converting energy of photons in UV-VIS light into the electric current. A metalorganic complex absorbing photons of certain energy is a 'photosensitizer'. Careful selection of the photosensitizers allows to effectively harvest photons of all energies in the UV-VIS range. The most known and effective photosensitizers to date are RuBPy and its derivatives [34].

However, copper(I) complexes with bispyrydyl are easily obtainable and effective models for these processes [35]. Their choice was also dictated by the fact, that MLCT in Cu(I) complex would result in creation of the Cu^{2+} species, and that should induce a significant change of the coordination geometry around Cu cation: from tetrahedral, characteristic

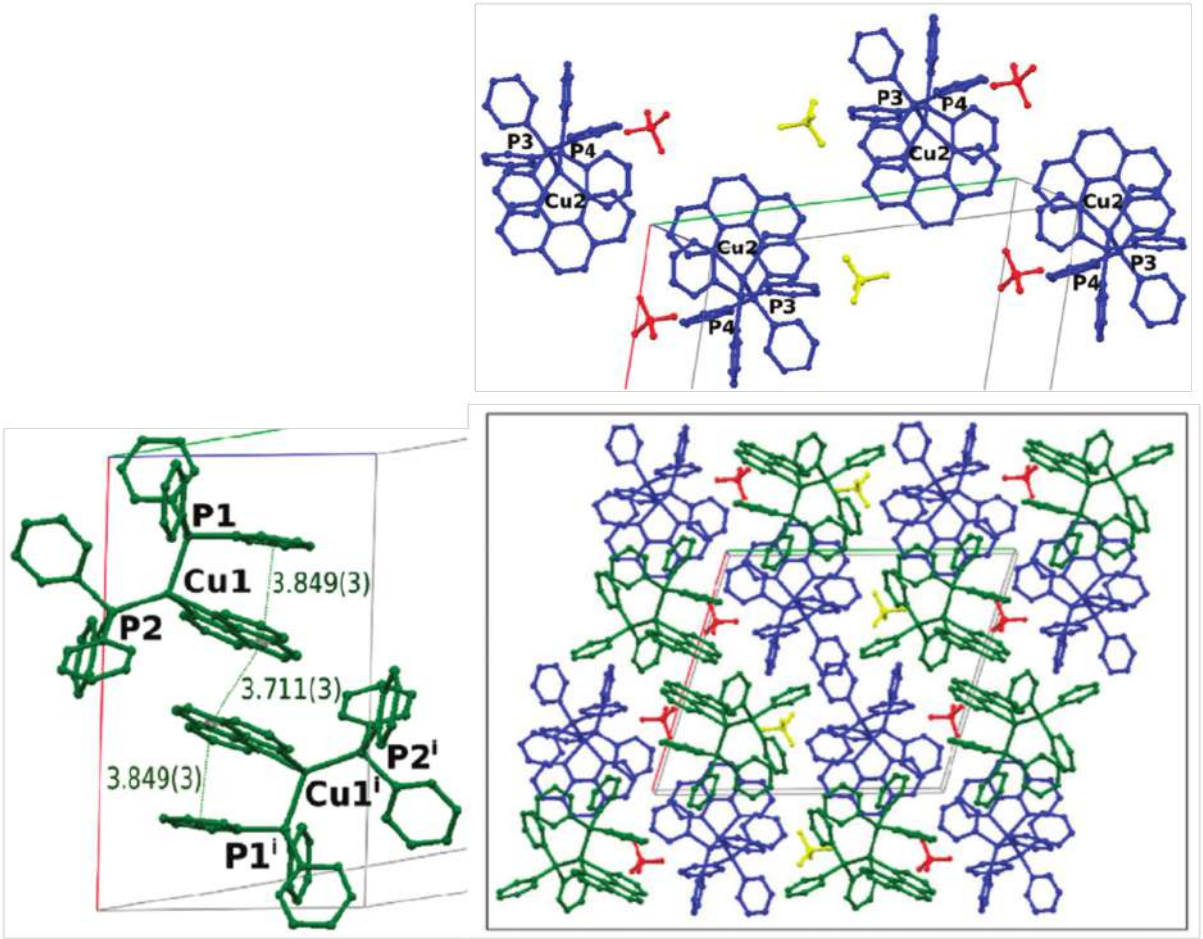

Figure 6: The crystal packing of CuBF4. The two crystallographically distinct complexes represented in green - **Cu(1)** and blue - **Cu(2)**. The interplanar distances between the phenantroline moieties in Å. H-atoms omitted for clarity. (Fig. 5 in [H5])

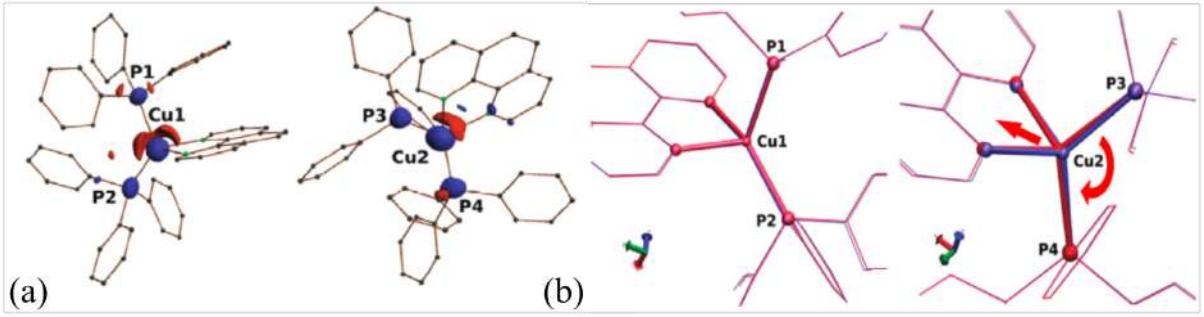

Figure 7: (a) The photodifference type-II map for the **Cu(1)** and **Cu(2)** moieties at 90 K with isosurfaces (red - positive, blue - negative) of +/-0.25 eÅ^{-3}; (b) the structural changes in Cu geometry induced by photoexcitation (red ES structure, blue - GS structure) of CuBF4. (Fig. 2 and 6 in [H5])

for Cu(I), it should transform towards square planar characteristic for Cu^{2+}. Such structural change was predicted by theoretical calculations for isolated Cu(I)phenantroline complexes and to some extent observed by the group of prof. Coppens in their earlier experiments on Cu(I) compounds [36].

In the course of research summarized in works [H5, H6], the excited-state structures of [Cu(I)(1,10-phenanthroline-N,N')] cations in their crystalline BF_4^- salt (further denoted as CuBF4) were determined for the first time at 180 K and 90 K by single-pulse time-resolved synchrotron experiments using polychromatic Laue method.

The most interesting fact discovered once the excited state structures were known was that the two independent molecules in the crystal (Figure 6) showed very distinct distortions upon excitation, differing in both magnitude and direction. Different responses could only be attributed to a pronounced difference in the molecular environment of the two complexes.

In the ground-state structure of CuBF4 one of the metalorganic cations (further denoted as **Cu(1)**) formed close intermolecular interactions with its symmetry-related counterpart. A close π-stacking of the phenanthroline (i.e. electron-accepting) ligands was noted, already resulting in a slight deformation of the ideal tetrahedral coordination of Cu(I). The other metalorganic cation, (further denoted as **Cu(2)**), on the other hand, was found to form no close-contacts with other cations but to be effectively encased in BF_4^- counterions, which did not participate in the electronic excitation process.

At lowest temperature, in the case of 'interacting' **Cu(1)** species, the flattening deformation of the tetrahedral coordination of copper was hardly perceptible, and a displacement of the Cu1 atom roughly within the P–Cu–P plane and away from associated phenanthroline ligand was observed.

The 'isolated' **Cu(2)** species, on the other hand, showed significant (by several degrees) flattening of copper coordination sphere and a pronounced displacement of Cu2 atom toward the phenanthroline ligand. The flattening was as much pronounced, as could be expected to take place in a tight crystalline environment, as proved by theoretical calculations using QMMM approach. In the case of 'interacting' **Cu(1)** dimers any further change in the copper coordination would have to affect the π-stacking interactions. On the other hand, copper coordination enforced by intermolecular interactions and crystalline environment in 'interacting' species was closer to that of excited state to begin with.

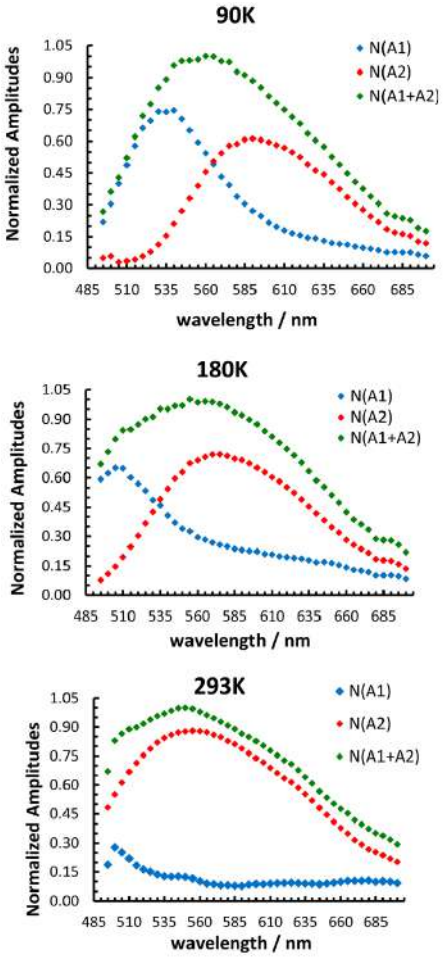

Figure 8: Luminescence spectra of CuBF4 at different temperatures (green), decomposed into two contributions with different excited state lifetimes, assigned to **Cu(1)** (red) and **Cu(2)** (blue) copper complexes. (Fig. 4 in [H6])

As the geometry of the excited states differed, the emission from the solid state CuBF4 was biexponential (Figure 8) with two distinct decay lifetimes. The longer-lived component, more prevalent as the temperature increased, was assigned to the more restricted molecule on the assumption, that a smaller structural change of the Cu(I)–phenanthroline complexes on excitation led to a longer lifetime of the excited species in agreement with earlier conclusions of McMillin et al. [37]. The more geometrically restricted species, with geometry fixed as slightly more convenient for the excitation would be more prone to remain in excited state for longer, while the 'unrestricted' species would encounter less hindrance in geometry relaxation from the crystal lattice - an effect more pronounced at higher temperatures.

Above all, the study illustrated emphatically that molecules in solids have physical properties different from those of isolated molecules, dependent on the specific molecular environment. This was the first case, where distinct behavior of two chemically identical species upon excitation in the solid state was proved to exist.

My contribution to these studies of CuBF4 [H5, H6] consisted of pointing out and characterizing the differences in crystalline environment of the two distinct species of CuBF4 in the crystal lattice, participation in data collection, processing of the data using in full the newly developed methods and proposing the final model of the excited state of CuBF4 for both of the independent species.

4.3.3 Luminescence of selected pyrene derivatives at high pressure

Policyclic Aromatic Hydrocarbons (PAHs) are objects of interest for instance due to their potential use in optoelectronics [41]. Among them, pyrene derivatives already show several interesting applications as electronic components [42, 43, 44, 45], charge transfer materials [46, 47], micellar probes [48, 49] or luminescent biomarkers [50, 51]. As a rule, luminescence of these compounds shows high sensitivity to environment [48, 52, 53] manifested in solvatochromism or upon attachment to biological macromolecules. In particular, molecular environment of a PAH encased in an aggregate (a dimer, a stack or a layer) will influence physicochemistry of such supramolecular construct. The ability of PAHs to form aggregates [54, 55] in solution as well as in thin films is vital to many of their applications.

In many instances aggregation of aromatic moieties in concentrated solution or in a crystal results in luminescence quenching. This appears to be the case of so called H-aggregates [56], i.e. parallel stacks of aromatic entities with significant π-orbital overlap

[57, 58]. However, there are also cases where certain modes of aggregation in the solid state enhanced luminescence of such compounds [55, 47].

Currently existing descriptions of the mechanism of PAH-s luminescence while in aggregates are hardly comprehensive. UV-VIS spectroscopy experiments: i.e. fluorescence band broadening, red-shifted and more unstructured emission spectra or characteristic fluorescence decay patterns are typical indicators of multimer formation upon excitation. However, such observations do not provide detailed information on structural changes, e.g. multiplicity of the excimers, neither at molecular nor at crystal lattice level. Such information can only be obtained indirectly by means of meticulous transient absorption studies or computational methods.

One way to gain control over intermolecular distances in a crystal is application of hydrostatic pressure. Structural analysis at high pressure can help explain physicochemical properties of materials thus analyzed, as presented e.g. in review works by Parsons [61], Fanetti [60] or Zakharov [62]. In particular, constricted crystalline environment may effectively enforce the presence of certain aggregates, which under standard conditions would be extremely short-lived and therefore hard to trace.

PAH-s and in particular pyrene derivatives at high pressure have not been extensively studied by X-ray diffraction so far. The works of Fabbiani et al. [63, 64] describe the structure evolution and phase transitions in naphtalene, anthracene and pyrene at pressures up to 2.1 GPa (naphtalene). On the other hand, a rare powder X-ray diffraction study by Capitani [65] carried out up to 25 GPa showed that phenantrene remained crystalline up to c.a. 20 GPa, undergoing phase transition around 8 GPa. A recent paper by Chanyshev et al. [66] deals with high-pressure and high-temperature-induced structural changes in benzene. In a wider perspective, a high-pressure study of organic conductor rubrene [67] showed that pressure-induced molecular rearrangement resulted in a phase transition and a loss of conducting properties of that material above 6 GPa.

My goal became to investigate the relationship between the packing of luminescent pyrene derivatives in the crystal lattice and their optical activity in the solid state. Flat aromatic fragments of these compounds tend to form stacks (π-stacking) in the crystal lattice; as a result, multimers of these compounds should be responsible for their solid state fluorescence. The first objective of my NCN–funded research project, which began in 2016, was to accumulate information on the solid-state photophysics of certain simple, model compounds. In these instances, the contribution to science was determination of missing links, such as crystal structures as well as solid-state spectroscopic properties.

Π-stacked pyreneladehyde and pyrene-allyl-ketone - model fluorescence enhancing aggregates of pyrene-based dyes

One of the simplest pyrene-based fluorophore containing an electron-donating substituent is pyrene-1-carbaldehyde (PA) (Figure 9a).

Its structure was first determined by Matsuzaki et. al. [68]. It has already been used as a component of Charge-Transfer Organic Cocrystals [47], where it was proved that its quantum efficiency of emission was increased by π-stacking in crystalline environment. The compound has also been known to show high sensitivity of fluorescence to its molecular environment in solution [53] and has been proposed as micelle probe based on its aggregation-dependent fluorescence color [48, 49].

In view of the these reports, it was surprising how little attention was paid to the emissive properties of a bulk PA itself. It made PA a promising object to investigate

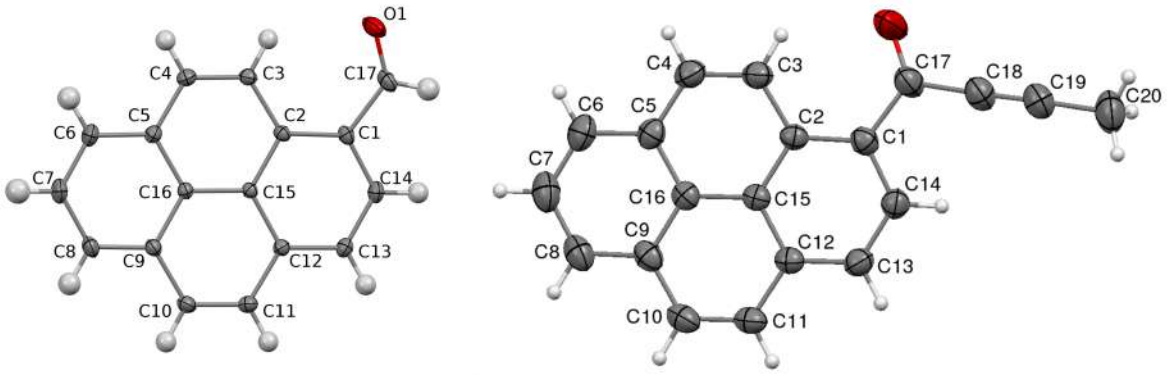

Figure 9: ORTEP representations of PA (at 100 K, left) and 1A (at 300 K, right) with labeling schemes. Hydrogen atoms inherit label number after the closest carbon atom. Atomic displacement parameters presented at 50% probability level.

the changes induced in its spectroscopic properties by crystalline environment and its rearrangements induced by pressure.

On the other hand, 1-(pyren-1-yl)but-2-yn-1-one (Figure 9b), further denoted as 1A has been recently found to display fluorescence quantum efficiency increased 6-fold in the solid state with respect to the solution [A12], with relatively long excited state lifetime. Time-resolved spectroscopy performed on powder sample suggested that such long-lived excited state is indeed the result of excimer formation, and that several types of excimers may be formed successively in the crystal. Small-size multimers (for instance dimers) were expected to form almost immediately, and than disappear, being incorporated into a more complicated excited multimers.

The works [H7] and [H8] covered structure determinations of PA and 1A by means of single-crystal X-ray diffraction at several pressures in range up to 3 GPa, combined with spectroscopic study in the solid state and supported by DFT calculations carried out in periodic conditions.

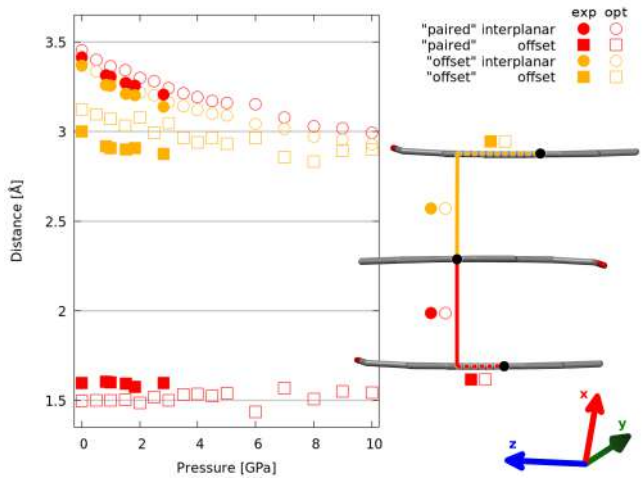

Figure 10: Vertical separation and horizontal shift observed for aromatic rings of "paired" and "offset" PA dimers in its crystal lattice. Filled markers indicate experimental results, hollow markers - the outcomes of theoretical geometry optimizations. (Fig. 6 from)[H7]

Prominent π-stacking of antiparallely oriented molecules and, to the lesser extent C–H$\cdots$O hydrogen bonds were found to determine crystal packing and its stability in the investigated conditions, confirming both PA and 1A as perfect models of pyrene-based aggregates. In particular, aromatic moieties stacking along the [100] direction were found to pair up within the π-stacks, and the pairing tendency was preserved across a wide pressure range (Figure 10 and Figure 6 in [H8]).

The most prominent difference in the structures of PA and 1A was in the angle at which pyrene moiety was inclined with respect to the stacking direction: in PA it was c. a. 0° while in 1A it was substantial, 75.5(5)°. In both instances the inclination of

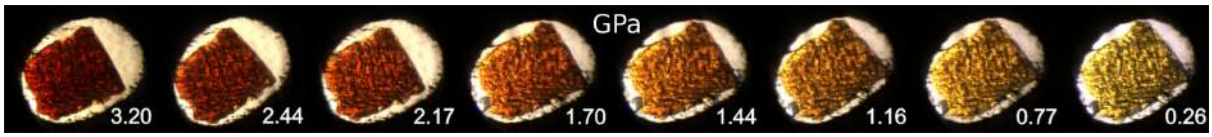

Figure 11: Microscopy images of a 1A crystal in a DAC (gasket diameter ≈400 μm, small ruby chip is visible at the lower-left corner. Gradual darkening of the sample with pressure indicates a red-shift in the UV-VIS absorption spectrum. This effect was repeatable and fully reversible. (Fig. 8 in [H8])

pyrene with respect to stacking direction did not vary with pressure. The stabilizing role of C–H$\cdots$O hydrogen in 1A was also much smaller.

A very good agreement between theoretically-optimized and experimentally-determined structures allowed to extend our analysis beyond experimentally attainable pressure range and link the most prominent features of crystal packing to electronic structure of PA and 1A.

Theoretically predicted shrinking of band-gap with pressure was well reflected in sample color changes (Figure 11 or Figure 10 in [H7]): the experimentally observed sample colors, strictly related to absorption λ_{max}, were in excellent agreement with their theoretical estimates.

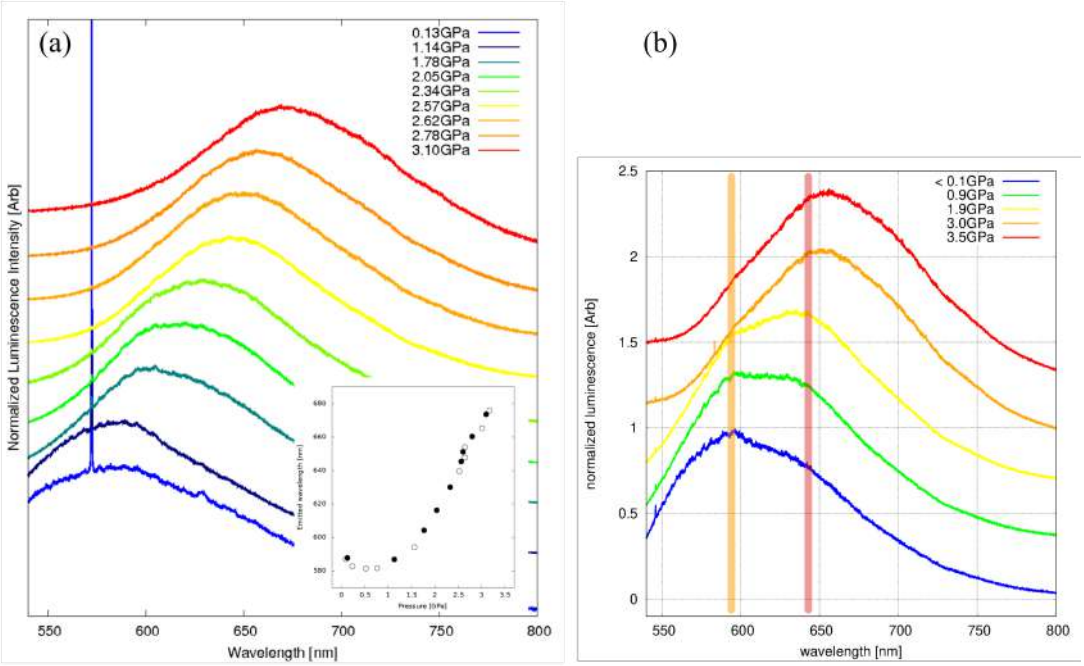

Figure 12: Luminescence spectra of (a) PA and (b) 1A at selected pressures. Excitation wavelength: 532nm. The spectra are normalized and offset along y-axis for clarity. Inset in (a) presents the change in position of experimental emission maxima with pressure (filled circles represent maxima of the spectra represented in the main figure). The orange and red bars indicate the emission maxima assigned to the initial small excimers and higher order multimers accordingly. (Fig. 11 in [H7] and Fig. 9 in [H8])

The fluorescence spectra of both PA and 1A showed a decided red-shift of the λ_{max}^{em} with pressure, as expected with the red-shift of maximal absorption wavelength (Figure 12). In both instances the average emission maxima increased almost linearly with pressure above 1 GPa and could be correlated with decrease in distance between the π-stacked pyrene moieties. The evolution of the emission spectra differed, however, in details. While in the case of PA fluorescence had one well-defined maximum irrespective

of pressure, in the case of 1A the emission band at low pressure appeared to consist of two components: one with maximum c.a. 597 nm ('orange band') and another, weaker, at about 635 nm ('red band'). As the pressure increased, the contribution of the 'red-band' became more prominent, and above 3.0 GPa the contribution from the 'orange band' was hardly noticeable.

In view of the former study [A12] the 'orange' band could be assigned to excitations occurring in fast-forming small aggregates of 1A, possibly originating from the very dimers that could be distinguished within the crystal structure. The 'red band' could then be assigned to excitations involving more complicated multimers. As the increased pressure forced molecules closer together, formation of the latter, many-component multimers could occur almost instantly, and emission from such multimers would dominate the spectrum.

It must be stressed however, that more definite statements concerning the electronic excitations in crystalline 1A could only be made based on a pressure-dependent time-resolved luminescence study, which would allow to compare luminescence decay-times of the 'orange' and 'red' bands, which I intend to perform in the future.

Due to our study [H7], the intense orange luminescence observed by Niko et. al [53] for frozen solution of PA could be unambiguously interpreted as a result of forming π-stacked aggregates, most probably π-stacked dimers, similar to the 'paired' interactions observed in the crystal structure of PA. Its increased efficiency may be attributed to blocking the vibrational relaxation pathways by tight crystal packing at higher pressures.

Methodology - handling highly incomplete diffraction data from high-pressure experiments

In order to investigate crystal structure of PA under pressure, one had to overcome the challenge posed by the very low symmetry of the analyzed system.

While Cambridge Structural Database (CSD 5.39, Ver. Nov. 2017 with updates covering year 2018) [69] contained c.a. 2000 structures determined at increased pressures, only 10% of them represented triclinic crystal system. Given that over 25% of all CSD depositions contain structures in triclinic system, and assuming the probability of a system being triclinic and investigated at high pressure were independent, binomial test predicts that the likelihood of such under-representation due to random chance (p-value) is less than 3.5^{-62}. The true reason for this under-representation of triclinic system is the challenge posed by structural analysis against highly incomplete data from high-pressure experiments performed in a diamond anvil cell (DAC).

The construction of diamond anvil cell (DAC) used to pressurize the sample (Figure 13a) heavily restricts the angles of both incident and diffracted X-ray beam, for which diffraction can be observed. An accessible volume of reciprocal space is limited to a thin disc, its thickness proportional to the cosine of the DAC opening angle [70]. In the case of a high pressure single-wavelength diffraction experiment on a triclinic crystal the expected data completeness from a standard DAC is very low (c.a. 31.17%). Experimental data is thus systematically incomplete, which leads to biased structural models.

The completeness can be increased, however, by placing several differently-oriented samples present in a single DAC (guaranteeing similar experimental conditions for all samples). The reciprocal space would then be probed by multiple differently-oriented discs (Figure 13), and according to our approximations the total completeness may near 56% for two and 74% for three crystals.

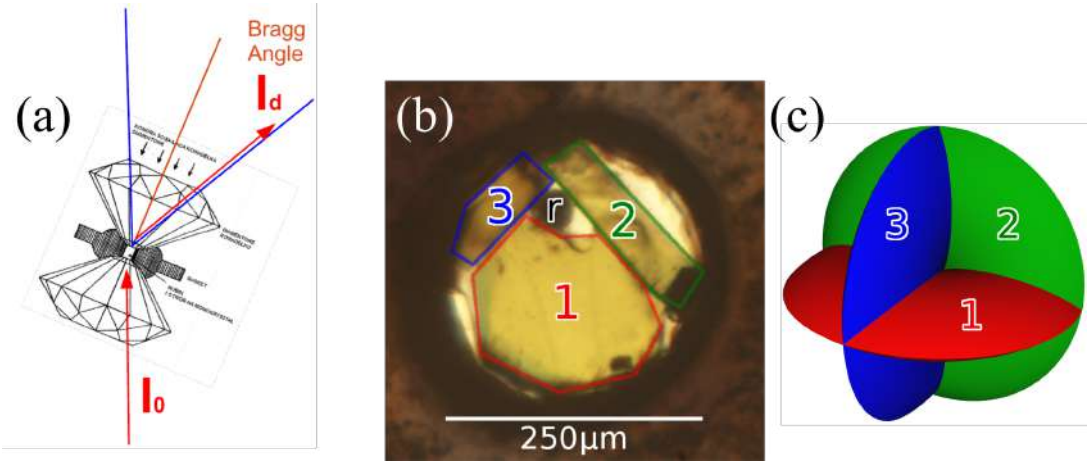

Figure 13: Schematic representation of a DAC, with opening cone marked in blue and the paths of the incident and diffracted beams marked in red. 'Multicrystal' approach adopted in [H7] (Fig. 2): b) the 3 crystals of PA loaded in a DAC, color-coded for clarity; 'r' indicates the reference ruby sphere c) a schematic representation of the parts of reciprocal space covered by diffraction from 3 crystals in ideal orientations.

The approach has its drawbacks. It is far more demanding both on preparation and processing stages, may introduce significant errors because of the need for appropriate scaling scheme, cause problems with absorption correction and inhomogeneity between samples. However, one of a few recent and cutting-edge cases where this challenging approach was applied, was the case of experimental charge density analysis performed on annulene above 6 GPa [71], where using two pre-oriented single crystals allowed to increase the overall data completeness to 88% (at 0.8 Å) in monoclinic system.

In the case of study on PA [H7], application of the multi-crystal approach allowed to obtain diffraction data of very satisfactory completeness (c.a. 70% up to 0.83 Å) for a low symmetry (triclinic) system at high pressure. Very adequate structural models, describing not only atomic coordinates, but also anisotropic displacement parameters of all non-H atoms and in excellent agreement with periodic DFT calculations were produced.

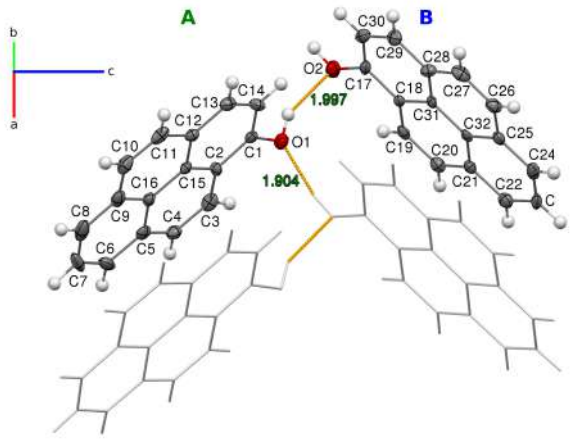

Figure 14: The 1-hydroxypyrene with its H-bond network.

Luminescence and mechanical properties of hydroxypyrene

In contrast to PA and 1A, 1-hydroxypyrene (pyrOH) is one of the simplest available pyrene derivatives capable of forming networks of strong H-bond and possessing electron-withdrawing substituent to pyrene moiety. It is luminescent in response to UV light, which made it a convenient marker in biochemical studies and its photophysics in solution have been thoroughly investigated [72]. Although preparation methods for this compound have been known for years [73, 52], its crystal structure has not been previously determined, nor were there any available studies concerning its photophysics in the solid state.

Our initial motivation was to investigate luminescent propensities of solid pyrOH and to determine its crystal structure both at ambient conditions and at high pressure. While preparing the samples for single crystal X-ray experiments, we observed that crystals of pyrOH displayed persistent habit (needle-shaped) irrespective of crystallization conditions (Figure 2 in [H9]). In addition, pyrOH showed strange behavior when recrystallized at non-ambient pressure (i.e. initially formed needle-shaped crystals would persist in growing only lengthwise, bending and breaking as a result). We decided to investigate the factors determining the conserved morphology of pyrOH crystals and its unique mechanical behavior. The work [H9] summarizes our efforts.

We determined the crystal structure of 1-hydroxypyrene for the first time, and characterized it over a wide temperature range. A bit surprisingly, pyrOH crystallized in a chiral $P2_1$ space group, with two independent molecules differing slightly in their orientation with respect to the main crystallographic direction. PyrOH formed stacks of parallel molecules, simultaneously stabilized by infinite chains of intermolecular H-bonds and π-stacking of pyrene moieties. The H-bond chains formed a unidirectional zig-zag pattern in the **bc** plane and bound stacks of pyrOH molecules in strongly-interacting double-columns along the screw-axis direction.

The whole structure can be considered as a relatively loosely bonded assemblage of parallel double-columns, as illustrated by interaction energies obtained from DFT calculations and, more graphically, by the energy frameworks [74] (Figure 8 in [H9]). As such, it turned out to be an example of a very anisotropic material, similar to crystalline aniline [60], but with a set of stronger H-bonds. Taking into account that the angles between pyrene planes and the stacking direction are wider than 32°, the crystal structure of pyrOH is a very nice model of an H-aggregate [56].

The very loosely interacting vertical motifs are reflected in conserved morphology of obtained single crystals, the needles being formed exactly along the direction of H-bonded π-stacks. High-pressure apparently increased the preference for pyrOH molecules to attach only to the existing stacks at the ends of already present crystallites.

H-bonds turned out to be the most rigid part of the crystal structure, with O...O distance resisting compression beyond $\approx$ 2.5Å and retaining small but stabilizing interaction energy up to 7.5 GPa. Such rigidity incorporated in a zig-zag pattern results in a significant compressibility of the system in [010] direction, compensated by almost no compression in the perpendicular [001] direction. The structure of pyrOH is therefore a fine example of a 'wine-rack mechanism' in the crystal lattice, a mechanism underlying negative linear compression (NLC) in several interesting inorganic and organometallic materials [75, 76, 77].

We successfully recorded steady-state fluorescence spectra of pyrOH at ambient conditions. It very closely resembles a spectra of 1-hydroxypyrene in water, with its discrete structure still partially discernible, maximum at 415nm, and additional small component at $\approx$ 500nm (Figure 15 in [H9]). The latter may be assigned to excimer formation in the solid state. From the relative intensity of the signals, it may be inferred that excimer formation is a minor event in the crystal, and the major response comes from individual molecules, similar to the case in solution. The observed fluorescence established pyrOH as one of the infrequent and interesting cases, where H-aggregation does not lead to fluorescence quenching.

4.3.4 Phase transition mechanism determined by crystalline environment

Molecular materials undergoing single-crystal-to-single-crystal (SCSC) phase transitions are of great interest to science and industry. Their spectroscopic [78], photoelectric [79], mechanic [80] or gas-storage [81] properties can be switched by controlled pressure or temperature changes without destroying crystallinity. It also means, that the structure of each phase can be investigated by single-crystal X-ray diffraction and a mechanism of such phase transition, vital for understanding the process and for new materials design, can be structurally probed, by means of systematic multi-temperature or multi-pressure diffraction experiments. Interestingly, in a number of recent studies on mechanisms of SCSC [82, 83, 84, 85, 86, 87] phase transitions were related to relatively small conformational changes of flexible aliphatic hydrocarbon chains.

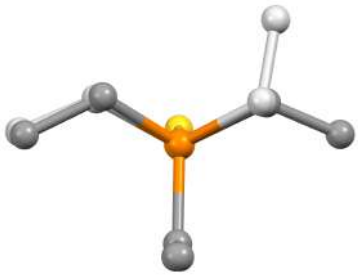

Figure 15: The overlay of the two most energetically stable conformations for triethylphosphine. View along the P–Metal bond. The conformation F indicated in dark grey and the conformation C in light grey. (Fig. 1 in [H10])

Triethylphosphine is a versatile ligand widely utilized in organometallic chemistry. With its three short aliphatic 'arms' it can be expected to exist in several conformations which do not differ significantly either in energy or an outward shape, a fact confirmed by both computational studies [88] and data mining of the Cambridge Structural Database [89]. Two conformations which are the most common in the CSD and the most energetically favorable are F and C conformations, represented in Figure 15. This makes the triethylphosphine a good candidate for a 'molecular switch'.

Although CSD database in 2018 contained over 2700 entries with triethylphosphine, only c.a. 50 (20 compounds) reported the existence of phase transitions or polymorphs. Among these, only 3 mentioned conformational changes of the triethylphosphine ligand [90, 91, 92] and none actually recounted phase transitions.

The lack of such reports suggested that the phenomenon od SCSC-s was either rare or overlooked because it would be undetectable in a standard single-temperature and single-pressure structure determination. In my opinion, it merited in-depth investigation.

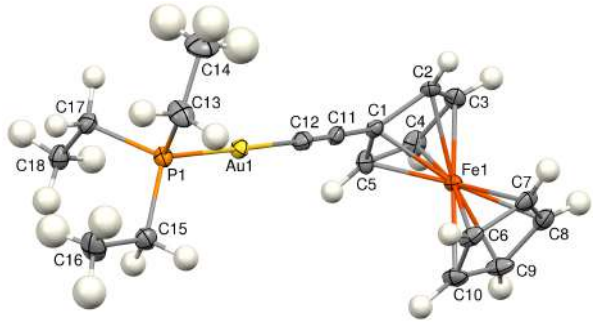

Figure 16: The molecule of compound FcPEt at 110 K, γ phase. Atomic displacement parameters represented at 50% probability level. Hydrogen atom numbers are the same as the numbers of connected C atoms. (Fig. 2 in [H10])

In work described in [H10] I concentrated on the newly-synthesized [A31] linear gold(I) complex (Figure 16), further denoted as FcPEt, which showed indications of two temperature-induced phase transitions, just above 125 K and 148 K.

The two phase transitions were discovered by the inspection of the unit cell parameters (Figure 4 in [H10]). In particular, the **c** lattice constant contracted by almost 0.2Å ($\approx$ 0.8% of its length) between 125 K and 140 K and by another 0.07Å between 140 K and 200 K. Consequently, the unit cell volume shrank by 0.6% between 125 K and 140 K, and, counter-intuitively at 200 K it was still smaller then at 110K.

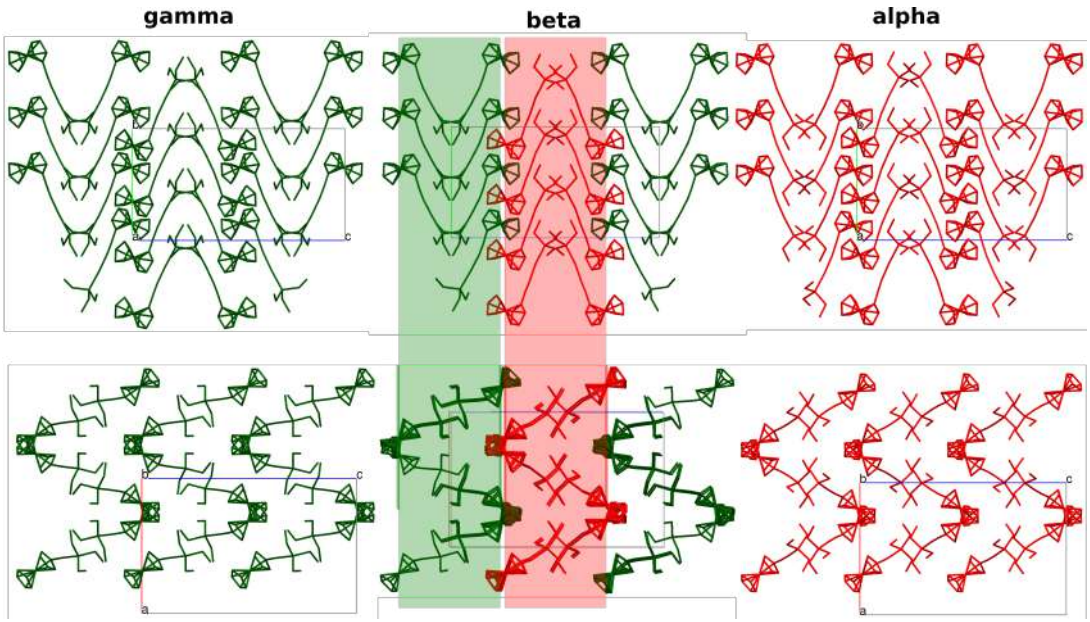

Figure 17: Comparison of the crystal packing of FcPEt at 110 K, γ phase (left, green), β phase at 140 K and α at 200 K (right, red), along [100] (a) and [010] (b) crystallographic directions. The symmetry-independent molecules in β phase colored according to the low-temperature (green) or high-temperature (red) conformation. H-atoms omitted for clarity.

The unit cell constants at all temperatures were consistent with orthorhombic crystal system. The systematic absences unambiguously suggested the centrosymmetric Pbca space group at 110 K, 125 K and 200K. However, at 140 K there were no systematic absences related to the c-glide plane in [010] direction (Figure 5 in [H10]). The structure of this phase has been ultimately solved in polar Pb21a space group, a subgroup of Pbca resulting directly from the c-glide plane removal.

Both in γ (below 125 K) and in α (above 150K) phase there was a single independent molecule of FcPEt in the crystallographic asymmetric unit, with overall geometry typical of linear gold(I) complexes [H10]. The triethylphosphine adopted the C conformation at low-temperature γ phase, but the most energetically stable F conformation at high-temperature α phase.

The major packing motif is a ribbon of FcPEt, related by crystallographic $b_{[100]}$ plane, stacked in [010] direction so that the adjacent ferrocene moieties are oriented almost perpendicularly to each other. These ribbons are then stacked on top of one another in crystallographic [100] and [001] directions, forming bands of Au–P–Et_3 fragments interspersed with bands of ferrocene moieties (Figure 17). The ethyl groups from PEt_3 in a band interact exclusively with other PEt_3 groups from molecules related by $a_{[001]}$, interlocking with them.

The crystal structure of FcPEt at 140 K, in the β phase, was a very specific intermediate between the low (γ) and high temperature (α) phases, giving a clue as to the mechanism of the observed phase transitions. There were two independent molecules in the asymmetric unit of FcPEt. While molecule 1 (m1) represented a conformation practically identical to that in the α phase, molecule 2 (m2) retained the the conformation of the γ phase (Figure 17). A view in [100] direction (Figure 17 middle) shows, that molecules m1 were restricted to every other band of Au–P–Et_3 fragments in the crystal in [001] direction, that is to the bands in which the PEt_3 moieties are in direct contact.

The reason for the contraction of the **c** parameter is very well illustrated in this view.

An average plane, containing all Fe atoms in a single molecular layer perpendicular to [001] can be drawn. The shortest distance between two such planes in a band containing molecules m1, which have already undergone a conformation change is shorter by over 0.1Å then the distance between the planes of molecules m2.

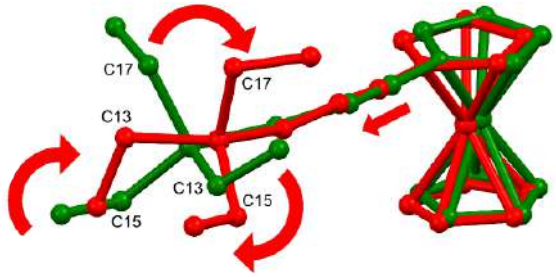

Figure 18: The overlay of molecules from the structure of FcPEt at 110 K (green) and 140 K (red), illustrating the exact structural change associated with the phase transition. (Fig. 10 in [H10])

Figure 18 represents a single m1 molecule overlaid on its low-temperature counterpart. The simplest way to transform the low-temperature m2 conformation into m1 would have to involve not only the flip of C13–C14 ethyl group, but also a rotation by $\approx 30^\circ$ of the whole phosphine along the axis of P–Au bond and conformational changes of the remaining two ethyl arms. The mechanism of the $\gamma \rightarrow \beta$ phase transition may be imagined as initiated by a rotation of a single PEt_3 group in a band (a single gear).

Conformation change of one or a few 'seeds', or isolated molecules of FcPEt, creates a chemical pressure [93, 94] in parts of the crystal lattice. Once enough steric strain is generated, the adjacent interlocked phosphines adjust their conformations, so the phase transition can be viewed as a series of connected gears rotating. Because a band of interacting phosphines consist of molecules related by the crystallographic $a_{[001]}$ plane, the analogy is even more to the point. Interlocking gears must rotate in opposite directions, and so the neighboring PEt_3 moieties, being mirror images of each other, fulfill this requirement.

The second, $\beta \rightarrow \alpha$ phase transition, above 140 K, restoring the initial Pbca symmetry, requires that molecules m2, in the hitherto unchanged layers, undergo an analogous sequential, molecular-gear driven conformation change.

A set of conditions for an ideal **crystalline geared lattice** has been proposed by Dominguez et. al. [95]: '... crystalline geared lattices will require systems with molecular rotors that experience steric contacts that constitute each other's main rotational barriers; geared rotors should also have matching cogs and rotational periods'. These conditions seem to be fulfilled exactly by the PEt_3 layered arrangement in FcPEt.

The proposed phase transition mechanism involves a structural change starting locally and propagating within well defined regions - bands - in the crystal lattice. It clearly resembles the processes of spin conversion in a broad family of spin-crossover complexes containing aliphatic alcohols as guests in crystal lattice [96, 97] or propagation of certain photoreactions in the solid state [94].

The temperature-related shrinking in [001] direction as a consequence of the consecutive rotations of PEt_3 moieties bears a resemblance to the concerted rotation of the rigid $FeCN_6$ octahedra underlying extreme compressibility of $LnFe(CN)_6$ under pressure [98]. This study discovered the triethylphosphine, a common ligand in organometallic chemistry, in a new role of a 'molecular gear', responsible for macroscopic properties of a material. Investigation of its impact on the propensities of other organometallic solids, especially the instances where crystalline environment allows for direct interaction of several PEt_3 moieties, will be attempted.

4.3.5 Summary

The above collection of publications covers my scientific achievements in photocrystallography, non-ambient (high-pressure) crystallography and in tracking Single-Crystal-to-Single-Crystal phase transitions, representing research in some of the more challenging sub-fields of crystallography. They all stress the need to reach beyond the description of a static molecular structure and represent the importance of considering the crystalline environment and its determining influence on the properties of a molecular species within a bulk. They all aim at explaining macroscopic physicochemical properties of analyzed materials on the basis of their crystal structures, and as such are contributions of some use to materials sciences. Finally, they all required performing experiments at non-standard conditions (either under excitation by UV light, at very high pressure or in the vicinity of phase transitions) and in some cases necessarily involved methods development.

My personal achievements can be summarized as:

* the first successful determination of the structure of short-lived excited state of metalorganic Rh(I) complex by application of synchrotron radiation and a challenging Laue (multi-wavelength) X-ray diffraction technique; [H1, H2],

* proposing and using effective procedures for retrieving information from several highly incomplete diffraction datasets from Laue experiments by preforming repeatable data collections, properly scaling data from different crystal samples and calculating photodifference maps tailored for the purpose of Laue experiments and use of the Ratio method [H1, H2],

* inspiring new fast and X-ray-wavelength-independent approach for Laue diffraction data indexing and participation in development of new methods and tools for X-ray data indexing and integration in photocrystallographic Laue experiments; the tools made it possible to perform short, preliminary experiments at the synchrotron and to optimize the conditions of photocrystallographic experiments [H3, H4],

* first-time structure determination of a short-lived excited state of Cu(I) compound in the crystal lattice, where structural changes upon excitation and resulting luminescence responses of two chemically identical molecules were different and highly dependent on their distinct crystalline environment [H5, H6],

* characterization of the structure - luminescence relationship for a set of simple pyrene derivatives bearing electron-donating substituents, where the tendency to form infinite π-stacks of antiparallel molecules with significant overlap of π fragments correlated with enhanced luminescence in the solid state, and showing crystal packing of these compounds as effective models of luminescent aggregates [H7, H8],

* presenting hydroxypyrene as a rare example of an H-aggregate being luminescent in the solid state, and an interesting case of a H-bond based 'wine-rack mechanism' in the crystal lattice, leading in extreme cases to negative linear compression (NLC) [H9],

* determination of the mechanism of a sequence of Single-Crystal-to-Single-Crystal phase transitions and establishing triethylphosphine as a molecular fragment which in proper crystalline environment can act as a 'molecular gear' [H10].

4.3.6 References

[1] William Henry Bragg and William Lawrence Bragg. The structure of the diamond. *Proceedings of the Royal Society of London. Series A, Containing Papers of a Mathematical and Physical Character*, 89(610):277–291, 1913.

[2] R. B. Woodward, M. Rosenblum, and M. C. Whiting. A new aromatic system. *Journal of the American Chemical Society*, 74(13):3458–3459, 1952.

[3] Philip Frank Eiland and Ray Pepinsky. X-ray examination of iron biscyclopentadienyl. *Journal of the American Chemical Society*, 74(19):4971–4971, 1952.

[4] J. D. Dunitz and L. E. Orgel. Bis-cyclopentadienyl iron: a molecular sandwich. *Nature*, 171(4342):121–122, 1953.

[5] Dorothy Crowfoot Hodgkin, Jennifer Kamper, Maureen Mackay, Jenny Pickworth, Kenneth N. Trueblood, and John G. White. Structure of Vitamin B 12. *Nature*, 178(4524):64, July 1956.

[6] J. C. Kendrew, R. E. Dickerson, B. E. Strandberg, R. G. Hart, D. R. Davies, D. C. Phillips, and V. C. Shore. Structure of Myoglobin: A Three-Dimensional Fourier Synthesis at 2 Å. Resolution. *Nature*, 185(4711):422, February 1960.

[7] M. F. Perutz, M. G. Rossmann, Ann F. Cullis, Hilary Muirhead, Georg Will, and A. C. T. North. Structure of Hæmoglobin: A Three-Dimensional Fourier Synthesis at 5.5-Å. Resolution, Obtained by X-Ray Analysis. *Nature*, 185(4711):416, February 1960.

[8] J. M. Bijvoet, A. F. Peerdeman, and A. J. van Bommel. Determination of the Absolute Configuration of Optically Active Compounds by Means of X-Rays. *Nature*, 168(4268):271, August 1951.

[9] S. J. L. Billinge, Th. Proffen, V. Petkov, J. L. Sarrao, and S. Kycia. Evidence for charge localization in the ferromagnetic phase of $la_{1-x}ca_xmno_3$ from high real-space-resolution x-ray diffraction. *Phys. Rev. B*, 62:1203–1211, Jul 2000.

[10] J. M. Hudspeth, D. J. Goossens, and T. R. Welberry. Approaches to modelling thermal diffuse scattering in triglycine sulfate, $(NH_2CH_2COOH)_3{\cdot}H_2SO_4$. *Journal of Applied Crystallography*, 47(2):544–551, Apr 2014.

[11] Mette S. Schmokel, Radoslaw Kaminski, Jason B. Benedict, and Philip Coppens. Data scaling and temperature calibration in time-resolved photocrystallographic experiments. *ACTA CRYSTALLOGRAPHICA SECTION A*, 66(6):632–636, NOV 2010.

[12] Philip Coppens, Jason Benedict, Marc Messerschmidt, Irina Novozhilova, Tim Graber, Yu-Sheng Chen, Ivan Vorontsov, Stephan Scheins, and Shao-Liang Zheng. Time-resolved synchrotron diffraction and theoretical studies of very short-lived photo-induced molecular species. *ACTA CRYSTALLOGRAPHICA SECTION A*, 66(2):179–188, MAR 2010.

[13] Hervé Cailleau, Maciej Lorenc, Laurent Guérin, Marina Servol, Eric Collet, and Marylise Buron-Le Cointe. Structural dynamics of photoinduced molecular switching in the solid state. *Acta Crystallographica Section A*, 66(2):189–197, Mar 2010.

[14] Philip Coppens, Mateusz Pitak, Milan Gembicky, Marc Messerschmidt, Stephan Scheins, Jason Benedict, Shin-ichi Adachi, Tokushi Sato, Shunsuke Nozawa, Kohei Ichiyanagi, Matthieu Chollet, and Shin-ya Koshihara. The RATIO method for time-resolved Laue crystallography. *JOURNAL OF SYNCHROTRON RADIATION*, 16:226–230, MAR 2009.

[15] Philip Coppens, Radoslaw Kaminski, and Mette S. Schmokel. On R factors for dynamic structure crystallography. *ACTA CRYSTALLOGRAPHICA SECTION A*, 66(5):626–628, SEP 2010.

[16] Ivan Vorontsov, Sebastien Pillet, Radoslaw Kaminski, Mette S. Schmokel, and Philip Coppens. LASER - a program for response-ratio refinement of time-resolved diffraction data. *JOURNAL OF APPLIED CRYSTALLOGRAPHY*, 43(5):1129–1130, OCT 2010.

[17] R. Bolotovsky and P. Coppens. The 'Seed-Skewness' Method for Integration of Peaks on Imaging Plates II. Analysis of Bias Due to Finite Size of the Peak Mask and Treatment of α_1-α_2 Splitting. *Journal of Applied Crystallography*, 30(3):244–253, Jun 1997.

[18] Philip Coppens, Shao-Liang Zheng, Milan Gembicky, Marc Messerschmidt, and Paulina M. Dominiak. Supramolecular solids and time-resolved diffraction. *CRYSTENGCOMM*, 8(10):735–741, 2006.

[19] Shao-Liang Zheng, Milan Gembicky, Marc Messerschmidt, and Philip Coppens. Ligand-tuning of the Excitation Wavelength of a Solid State E/Z Isomerization: [Zn(TA)(2)(2,2 '-bipyridyl)] in a Supramolecular Framework. *JOURNAL OF THE CHINESE CHEMICAL SOCIETY*, 56(1):16–21, FEB 2009.

[20] Shao-Liang Zheng, Milan Gembicky, Marc Messerschmidt, Paulina M. Dominiak, and Philip Coppens. Effect of the environment on molecular properties: Synthesis, structure, and photoluminescence of Cu(I) bis(2,9-dimethyl-1,10-phenanthroline) nanoclusters in eight different supramolecular frameworks. *INORGANIC CHEMISTRY*, 45(23):9281–9289, NOV 13 2006.

[21] Philip Coppens, Oksana Gerlits, Ivan I. Vorontsov, Andrey Yu. Kovalevsky, Yu-Sheng Chen, Tim Graber, Milan Gembicky, and Irina V. Novozhilova. A very large rh–rh bond shortening on excitation of the [rh2(1,8-diisocyano-p-menthane)4]2+ ion by time-resolved synchrotron x-ray diffraction. *Chem. Commun.*, pages 2144–2145, 2004.

[22] Philip Coppens, Ivan I. Vorontsov, Tim Graber, Milan Gembicky, and Andrey Yu. Kovalevsky. The structure of short-lived excited states of molecular complexes by time-resolved x-ray diffraction. *Acta Crystallographica Section A*, 61(2):162–172.

[23] Joel T. Mague. Conformational diversity in the solid state structures of [rh2(mu-ch3n(p(och3)2)2)2(ch3n(p(och3)2)2)2]x2 (x = o3scf3, b(c6h5)4). *Inorganica Chimica Acta*, 229(1):17 – 25, 1995.

[24] Richard L. Blakley, Yan Yin, Charles Lloyd, Joel T. Mague, and Gary L. McPherson. Photophysics of a flexible ligand bridged rhodium(i) dimer: An excited state conformational change in a crystalline solid. *Chemical Physics Letters*, 157(5):398 – 402, 1989.

[25] Ivan I. Vorontsov and Philip Coppens. On the refinement of time-resolved diffraction data: comparison of the random-distribution and cluster-formation models and analysis of the light-induced increase in the atomic displacement parameters. *Journal of Synchrotron Radiation*, 12(4):488–493.

[26] Radoslaw Kaminski, Mette S. Schmokel, and Philip Coppens. Constrained Excited-State Structure in Molecular Crystals by Means of the QM/MM Approach: Toward the Prediction of Photocrystallographic Results. *JOURNAL OF PHYSICAL CHEMISTRY LETTERS*, 1(15):2349–2353, AUG 5 2010.

[27] Philip Coppens and Bertrand Fournier. On the scaling of multicrystal data sets collected at high-intensity X-ray and electron sources. *STRUCTURAL DYNAMICS*, 2(6), NOV 2015.

[28] Bertrand Fournier, Jesse Sokolow, and Philip Coppens. Analysis of multicrystal pump-probe data sets. II. Scaling of ratio data sets. *ACTA CRYSTALLOGRAPHICA A-FOUNDATION AND ADVANCES*, 72(2):250–260, MAR 2016.

[29] Katarzyna N. Jarzembska, Radoslaw Kaminski, Bertrand Fournier, Elzbieta Trzop, Jesse D. Sokolow, Robert Henning, Yang Chen, and Philip Coppens. Shedding Light on the Photochemistry of Coinage-Metal Phosphorescent Materials: A Time-Resolved Laue Diffraction Study of an Ag-I-Cu-I Tetranuclear Complex. *INORGANIC CHEMISTRY*, 53(19):10594–10601, OCT 6 2014.

[30] Katarzyna N. Jarzembska, Michal Hapka, Radoslaw Kaminski, Wojciech Bury, Sylwia E. Kutniewska, Dariusz Szarejko, and Malgorzata M. Szczesniak. On the Nature of Luminescence Thermochromism of Multinuclear Copper(I) Benzoate Complexes in the Crystalline State. *CRYSTALS*, 9(1), JAN 2019.

[31] William H. Kruskal and W. Allen Wallis. Use of ranks in one-criterion variance analysis. *Journal of the American Statistical Association*, 47(260):pp. 583–621, 1952.

[32] Gregory W. Corder and Dale I. Foreman. *Nonparametric Statistics for Non-Statisticians.* John Wiley & Sons, Inc, 2009.

[33] Soille Pierre. *Morphological Image Analysis; Principles and Applications.* Springer, 2003.

[34] Yong-Jun Yuan, Zhen-Tao Yu, Da-Qin Chen, and Zhi-Gang Zou. Metal-complex chromophores for solar hydrogen generation. *Chem. Soc. Rev.*, 46:603–631, 2017.

[35] Takeru Bessho, Edwin C. Constable, Michael Graetzel, Ana Hernandez Redondo, Catherine E. Housecroft, William Kylberg, Md. K. Nazeeruddin, Markus Neuburger, and Silvia Schaffner. An element of surprise—efficient copper-functionalized dye-sensitized solar cells. *Chem. Commun.*, pages 3717–3719, 2008.

[36] Ivan I. Vorontsov, Tim Graber, Andrey Yu. Kovalevsky, Irina V. Novozhilova, Milan Gembicky, Yu-Sheng Chen, and Philip Coppens. Capturing and Analyzing the Excited-State Structure of a Cu(I) Phenanthroline Complex by Time-Resolved Diffraction and Theoretical Calculations. *JOURNAL OF THE AMERICAN CHEMICAL SOCIETY*, 131(18):6566–6573, MAY 13 2009.

[37] Michèle K. Eggleston, David R. McMillin, Kristina S. Koenig, and Alexander J. Pallenberg. Steric effects in the ground and excited states of cu(nn)2+ systems. *Inorganic Chemistry*, 36(2):172–176, 1997.

[38] Jonathan V. Caspar, Edward M. Kober, B. Patrick Sullivan, and Thomas J. Meyer. Application of the energy gap law to the decay of charge-transfer excited states. *Journal of the American Chemical Society*, 104(2):630–632, 1982.

[39] Jonathan V. Caspar and Thomas J. Meyer. Application of the energy gap law to nonradiative, excited-state decay. *The Journal of Physical Chemistry*, 87(6):952–957, 1983.

[40] Karl F. Freed and Joshua Jortner. Multiphonon processes in the nonradiative decay of large molecules. *The Journal of Chemical Physics*, 52(12):6272–6291, 1970.

[41] JohnE. Anthony. The larger acenes: Versatile organic semiconductors. *Angewandte Chemie International Edition*, 47(3):452–483, 2008.

[42] Teresa M. Figueira-Duarte and Klaus Müllen. Pyrene-based materials for organic electronics. *Chemical Reviews*, 111(11):7260–7314, 2011.

[43] Zhi-Qiang Wang, Chuan-Lin Liu, Cai-Jun Zheng, Wei-Zhou Wang, Chen Xu, Mei Zhu, Bao-Ming Ji, Fan Li, and Xiao-Hong Zhang. Efficient violet non-doped organic light-emitting device based on a pyrene derivative with novel molecular structure. *Organic Electronics*, 23:179–185, August 2015.

[44] Shinaj K. Rajagopal, V. Sivaranjana Reddy, and Mahesh Hariharan. Crystallization induced green-yellow-orange emitters based on benzoylpyrenes. *CrystEngComm*, 18(27):5089–5094, July 2016.

[45] Shinaj K. Rajagopal, Ajith R. Mallia, and Mahesh Hariharan. Enhanced intersystem crossing in carbonylpyrenes. *Physical Chemistry Chemical Physics*, 19(41):28225–28231, October 2017.

[46] Maxim V. Ivanov, Khushabu Thakur, Anitha Boddeda, Denan Wang, and Rajendra Rathore. Nodal arrangement of homo controls the turning on/off the electronic coupling in isomeric polypyrene wires. *The Journal of Physical Chemistry C*, 121(17):9202–9208, 2017.

[47] Hao Sun, Jing Peng, Kun Zhao, Rabia Usman, Arshad Khan, and Mingliang Wang. Efficient Luminescent Microtubes of Charge-Transfer Organic Cocrystals Involving 1,2,4,5-Tetracyanobenzene, Carbazole Derivatives, and Pyrene Derivatives. *Crystal Growth & Design*, 17(12):6684–6691, December 2017.

[48] Ch. V. Kumar, S. K. Chattopadhyay, and P. K. Das. A laser flash photolysis study of pyrene-1-aldehyde. intersystem crossing efficiency, photoreactivity and triplet state properties in various solvents. *Photochemistry and Photobiology*, 38(2):141–152, 1983.

[49] J.M. Otón and A.U. Acuña. Fluorescence quantum yield of pyrene-1-carboxaldehyde in protic solvents. *Journal of Photochemistry*, 14(4):341 – 343, 1980.

[50] Enrico Faggi, Jenny Serra-Vinardell, Mrituanjay D. Pandey, Josefina Casas, Gemma Fabriàs, Santiago V. Luis, and Ignacio Alfonso. Pseudopeptidic fluorescent on-off ph sensor based on pyrene excimer emission: Imaging of acidic cellular organelles. *Sensors and Actuators B: Chemical*, 234:633 – 640, 2016.

[51] Ilya O. Aparin, Gleb V. Proskurin, Andrey V. Golovin, Alexey V. Ustinov, Andrey A. Formanovsky, Timofei S. Zatsepin, and Vladimir A. Korshun. Fine tuning of pyrene excimer fluorescence in molecular beacons by alteration of the monomer structure. *The Journal of Organic Chemistry*, 82(19):10015–10024, 2017.

[52] Manuela Petaccia, Luisa Giansanti, Francesca Leonelli, Angela La Bella, Denise Gradella Villalva, and Giovanna Mancini. Synthesis, characterization and inclusion into liposomes of a new cationic pyrenyl amphiphile. *Chemistry and Physics of Lipids*, 200:83 – 93, 2016.

[53] Yosuke Niko, Yuki Hiroshige, Susumu Kawauchi, and Gen-ichi Konishi. Fundamental photoluminescence properties of pyrene carbonyl compounds through absolute fluorescence quantum yield measurement and density functional theory. *Tetrahedron*, 68:6177–6185, 08 2012.

[54] G. R. Desiraju and A. Gavezzotti. Crystal structures of polynuclear aromatic hydrocarbons. Classification, rationalization and prediction from molecular structure. *Acta Crystallographica Section B: Structural Science*, 45(5):473–482, October 1989.

[55] Tomoaki Hinoue, Yuta Shigenoi, Misa Sugino, Yuji Mizobe, Ichiro Hisaki, Mikiji Miyata, and Norimitsu Tohnai. Regulation of pi-stacked anthracene arrangement for fluorescence modulation of organic solid from monomer to excited oligomer emission. *Chemistry – A European Journal*, 18(15):4634–4643, 2012.

[56] Shinto Varghese and Suresh Das. Role of molecular packing in determining solid-state optical properties of pi-conjugated materials. *The Journal of Physical Chemistry Letters*, 2(8):863–873, 2011. PMID: 26295620.

[57] N. S. Saleesh Kumar, Shinto Varghese, C. H. Suresh, Nigam P. Rath, and Suresh Das. Correlation between solid-state photophysical properties and molecular packing in a series of indane-1,3-dione containing butadiene derivatives. *The Journal of Physical Chemistry C*, 113(27):11927–11935, 2009.

[58] Suhrit Ghosh, Xue-Qing Li, Vladimir Stepanenko, and Frank Würthner. Control of h- and j-type pi stacking by peripheral alkyl chains and self-sorting phenomena in perylene bisimide homo- and heteroaggregates. *Chemistry – A European Journal*, 14(36):11343–11357, 2008.

[59] Espen Eikeland, Maja K. Thomsen, Jacob Overgaard, Mark A. Spackman, and Bo B. Iversen. Intermolecular interaction energies in hydroquinone clathrates at high pressure. *Crystal Growth & Design*, 17(7):3834–3846, 2017.

[60] Samuele Fanetti, Margherita Citroni, Kamil Dziubek, Marcelo Medre Nobrega, and Roberto Bini. The role of H-bond in the high-pressure chemistry of model molecules. *Journal of Physics: Condensed Matter*, 30(9):094001, 2018.

[61] Stephen Moggach and Simon Parsons. Molecular solids at extreme pressure. *CrystEngComm*, 12:2515–2515, 2010.

[62] Boris A. Zakharov and Elena V. Boldyreva. High pressure: a complementary tool for probing solid-state processes. *CrystEngComm*, pages –, 2019.

[63] Francesca P. A. Fabbiani, David R. Allan, William I. F. David, Stephen A. Moggach, Simon Parsons, and Colin R. Pulham. High-pressure recrystallisation—a route to new polymorphs and solvates. *CrystEngComm*, 6:505–511, 2004.

[64] Francesca P. A. Fabbiani, David R. Allan, Simon Parsons, and Colin R. Pulham. Exploration of the high-pressure behaviour of polycyclic aromatic hydrocarbons: naphthalene, phenanthrene and pyrene. *Acta Crystallographica Section B Structural Science*, 62(5):826–842, October 2006.

[65] F. Capitani, M. Höppner, L. Malavasi, C. Marini, G. A. Artioli, M. Hanfland, P. Dore, L. Boeri, and P. Postorino. Structural Evolution of Solid Phenanthrene at High Pressures. *The Journal of Physical Chemistry C*, 120(26):14310–14316, July 2016.

[66] Artem D. Chanyshev, Konstantin D. Litasov, Sergey V. Rashchenko, Asami Sano-Furukawa, Hiroyuki Kagi, Takanori Hattori, Anton F. Shatskiy, Anna M. Dymshits, Igor S. Sharygin, and Yuji Higo. High-Pressure–High-Temperature Study of Benzene: Refined Crystal Structure and New Phase Diagram up to 8 GPa and 923 K. *Crystal Growth & Design*, 18(5):3016–3026, May 2018.

[67] Stefano Bergantin, Massimo Moret, Gernot Buth, and Francesca P. A. Fabbiani. Pressure-Induced Conformational Change in Organic Semiconductors: Triggering a Reversible Phase Transition in Rubrene. *The Journal of Physical Chemistry C*, 118(25):13476–13483, June 2014.

[68] Sanae Y. Matsuzaki, Midori Goto, Kazumasa Honda, and Isao Kojima. Crystal and Molecular Structures of 1-Pyrenecarbaldehyde. *Analytical Sciences*, 11:461–463, June 1995.

[69] C. R. Groom, I. J. Bruno, M. P. Lightfoot, and S. C. Ward. The Cambridge Structural Database. *Acta Crystallographica Section B*, 72(2):171–179, April 2016.

[70] Leo Merrill and William A. Bassett. Miniature diamond anvil pressure cell for single crystal x-ray diffraction studies. *Review of Scientific Instruments*, 45(2):290–294, 1974.

[71] Nicola Casati, Annette Kleppe, Andrew P. Jephcoat, and Piero Macchi. Putting pressure on aromaticity along with in situ experimental electron density of a molecular crystal. *Nature Communications*, 7:10901, March 2016.

[72] B. H. Milosavljevic and J. K. Thomas. The photophysics of 1-hydroxypyrene, the acidity of its singlet excited state, and the nature of its photoionization process in polar media. *Photochem. Photobiol. Sci.*, 1:100–104, 2002.

[73] Raj K. Sehgal and Subodh Kumar. A simple preparation of 1-hydroxypyrene. *Organic Preparations and Procedures International*, 21(2):223–225, 1989.

[74] Campbell F. Mackenzie, Peter R. Spackman, Dylan Jayatilaka, and Mark A. Spackman. CrystalExplorer model energies and energy frame-works: extension to metal coordination compounds, organic salts, solvates and open-shell systems. *Iucrj*, 4:575–587, September 2017.

[75] Weizhao Cai and Andrzej Katrusiak. Giant negative linear compression positively coupled to massive thermal expansion in a metal–organic framework. *Nature Communications*, 5:4337, July 2014.

[76] Andrew B. Cairns, Jadna Catafesta, Claire Levelut, Jerome Rouquette, Arie van der Lee, Lars Peters, Amber L. Thompson, Vladimir Dmitriev, Julien Haines, and Andrew L. Goodwin. Giant negative linear compressibility in zinc dicyanoaurate. *Nature Materials*, 12(3):212–216, March 2013.

[77] Andrew L. Goodwin, David A. Keen, and Matthew G. Tucker. Large negative linear compressibility of ag3[co(cn)6]. *Proceedings of the National Academy of Sciences*, 105(48):18708–18713, 2008.

[78] Larry R. Falvello, Michael A. Hitchman, Fernando Palacio, Isabel Pascual, Arthur J. Schultz, Horst Stratemeier, Milagros Tomás, Esteban P. Urriolabeitia, and Dianna M. Young. Tunable molecular distortion in a nickel complex coupled to a reversible phase transition in the crystalline state. *Journal of the American Chemical Society*, 121(12):2808–2819, 1999.

[79] Lina Li, Zhihua Sun, Chengmin Ji, Sangen Zhao, and Junhua Luo. Rational design and syntheses of molecular phase transition crystal materials. *Crystal Growth & Design*, 16(12):6685–6695, 2016.

[80] Elisa Nauha, Pance Naumov, and Matteo Lusi. Fine-tuning of a thermosalient phase transition by solid solutions. *CrystEngComm*, 18:4699–4703, 2016.

[81] Jarad A. Mason, Julia Oktawiec, Mercedes K. Taylor, Matthew R. Hudson, Julien Rodriguez, Jonathan E. Bachman, Miguel I. Gonzalez, Antonio Cervellino, Antonietta Guagliardi, Craig M. Brown, Philip L. Llewellyn, Norberto Masciocchi, and Jeffrey R. Long. Methane storage in flexible metal–organic frameworks with intrinsic thermal management. *Nature*, 527(7578):357–361, November 2015.

[82] M. Castro, L. R. Falvello, E. Forcén-Vázquez, P. Guerra, N. A. Al-Kenany, G. Martínez, and M. Tomás. A phase transition caught in mid-course: independent and concomitant analyses of the monoclinic and triclinic structures of (nBu4n)[Co(orotate)2(bipy)]·3h2o. *Acta Crystallographica Section C*, 73(9):731–742, September 2017.

[83] A. Katrusiak. Conformational transformation coupled with the order–disorder phase transition in 2-methyl-1,3-cyclohexanedione crystals. *Acta Crystallographica Section B*, 56(5):872–881, October 2000.

[84] D. Hashizume, N. Miki, T. Yamazaki, Y. Aoyagi, T. Arisato, H. Uchiyama, T. Endo, M. Yasui, and F. Iwasaki. Mechanism of the first-order phase transition of an acylurea derivative: observation of intermediate stages of transformation with a detailed temperature-resolved single-crystal diffraction method. *Acta Crystallographica Section B*, 59(3):404–415, June 2003.

[85] M. M. H. Smets, S. J. T. Brugman, E. R. H. van Eck, P. Tinnemans, H. Meekes, and H. M. Cuppen. Understanding the single-crystal-to-single-crystal solid-state phase transition of dl -methionine. *CrystEngComm*, 18(48):9363–9373, 2016.

[86] Tatiana N. Drebushchak, Yury A. Chesalov, and Elena V. Boldyreva. A conformational polymorphic transition in the high-temperature ε-form of chlorpropamide on cooling: a new ε'-form. *Acta Crystallographica Section B*, 65(6):770–781, Dec 2009.

[87] Tatiana N. Drebushchak, Valeri A. Drebushchak, and Elena V. Boldyreva. Solid-state transformations in the β-form of chlorpropamide on cooling to 100K. *Acta Crystallographica Section B*, 67(2):163–176, Apr 2011.

[88] Nuwan De Silva, Federico Zahariev, Benjamin P. Hay, Mark S. Gordon, and Theresa L. Windus. Conformations of Organophosphine Oxides. *The Journal of Physical Chemistry A*, 119(32):8765–8773, August 2015.

[89] Dianne D. Ellis, Mairi F. Haddow, A. Guy Orpen, and Paul J. Watson. Conformational analysis of PEt3 and P(OMe)3 in metal complexes. *Dalton Transactions*, (47):10436–10445, 2009.

[90] Audrey A. Cole, James C. Fettinger, D. Webster Keogh, and Rinaldo Poli. Dissociative phosphine exchange for cyclopentadienylmolybdenum(III) systems. Bridging the gap between Werner-like coordination chemistry and low-valent organometallic chemistry. *Inorganica Chimica Acta*, 240(1):355–366, December 1995.

[91] A. Asgar Torabi, Anthony S Humphreys, George A Koutsantonis, Brian W Skelton, and Allan H White. Phosphine substituted Ru3(mu-dppm)(CO)10: structural trends within [Ru3(mu-dppm)(PR3)(CO)9] (R=Et, Ph, Cy and Pri). *Journal of Organometallic Chemistry*, 655(1):227–232, August 2002.

[92] Fernande D. Rochon, Robert Melanson, and Pi-Chang Kong. Synthesis and Crystal Structure of a New Type of Ionic Technetium(V) Dioxo Phosphine Complexes, [Tc(O)2(PR3)3]+. Reactions with Pyridine and Crystal Structures of trans,cis,cis-[Tc(O)2(PR3)2(py)2]+ Compounds. *Inorganic Chemistry*, 37(1):87–92, January 1998.

[93] Tadeusz Luty and René Fouret. On stability of molecular solids "under chemical pressure". *The Journal of Chemical Physics*, 90(10):5696–5703, May 1989.

[94] N. M. Peachey and C. J. Eckhardt. Energetics of organic solid-state reactions: lattice dynamics and chemical pressure in the 2,5-distyrylpyrazine photoreaction. *The Journal of Physical Chemistry*, 97(41):10849–10856, 1993.

[95] Zaira Dominguez, Hung Dang, M. Jane Strouse, and Miguel A. Garcia-Garibay. Molecular "compasses" and "gyroscopes." iii. dynamics of a phenylene rotor and clathrated benzene in a slipping-gear crystal lattice. *Journal of the American Chemical Society*, 124(26):7719–7727, 2002.

[96] Karl W. Törnroos, Marc Hostettler, Dmitry Chernyshov, Brita Vangdal, and Hans-Beat Bürgi. Interplay of Spin Conversion and Structural Phase Transformations: Re-Entrant Phase Transitions in the 2-Propanol Solvate of Tris(2-picolylamine)iron(II) Dichloride. *Chemistry – A European Journal*, 12(24):6207–6215, July 2006.

[97] Dmitry Chernyshov, Nikolay Klinduhov, Karl W. Törnroos, Marc Hostettler, Brita Vangdal, and Hans-Beat Bürgi. Coupling between spin conversion and solvent disorder in spin crossover solids. *Phys. Rev. B*, 76:014406–3–014406–7, Jul 2007.

[98] Samuel G. Duyker, Vanessa K. Peterson, Gordon J. Kearley, Andrew J. Studer, and Cameron J. Kepert. Extreme compressibility in lnfe(cn)6 coordination framework materials via molecular gears and torsion springs. *Nature Chemistry*, 8:270–275, Jan 2016.

5 OTHER SCIENTIFIC ACHIEVEMENTS

5.1 SCIENTIFIC INTERESTS

5.1.1 Experimental Charge Density Analysis

My PhD thesis concentrated on experimental charge density analysis for organometallic compounds obtained from the refinement of the multipole electron density model using the results of high-resolution X-ray measurements [A3]. I continue to work in the field. In particular, I am interested in estimating the strength and relative importance of the intermolecular interactions in the crystal structures. Shortly after obtaining my PhD, I was able to classify, using topological experimental electron density, intermolecular interactions for several Schiff bases, and link their properties to the NMR results [A2]. More recently, I supervised a comparative experimental charge density analyses on a popular antibiotic doxycycline in both the zwitterionic monohydrate and the protonated hydrochloride crystal forms [A35]. I also initiated another study, combining experimental charge density analysis with analysis of intermolecular interaction energies in the crystal structures of the popular analgesic and anti-inflammatory drug ketoprophen [A33].

5.1.2 Interpretation of Diffuse Scattering

I had an opportunity to participate in the work on the interpretation of diffuse scattering and its use to more accurately describe the structures of organic compounds [A19]. Interpretation of signals other than Bragg's reflections recorded in diffraction experiments is a new field of crystallography, which is of great significance in materials research, as a means to explain the mechanisms underlying superconductivity or ferroelectricity. In this particular case the model organic salt (N-(3-(2,6-dimethylanilino)-1-methylbut-2-enylidene)-2,6-dimethylanilinium chloride) was not a known functional material, but was the case in which careful interpretation of diffuse scattering was indispensable to determine chemically reasonable structural model and to identify the proper symmetry in the crystal. Going beyond interpretation of Bragg intensities allowed to classify this structure as a collection of weakly interacting 'rods', the weak interactions resulting in relative shifts of such rods within the crystal and in an elaborate domain structure of the material.

5.1.3 Crystal structure analysis for luminescent materials

Owing to collaboration with the groups of prof. dr hab. Janusz Zakrzewski and dr hab. Damian Plażuk from the University of Lódź, I have continuous opportunities to discover crystal structures for a broad range of organic and organometallic luminescent materials, e.g. in [A12, A36, A31, A37]. As already stated, these compounds are of interest due to relatively high fluorescence quantum yields (up to 60%) and various possibilities of modifying the emission wavelength of the material by simple structural modifications its components of pyrene (perylene, naphtalene) or by inducing polymorphism and designing crystal forms most suitable for applications as luminophores. Reliable structural analysis is an indispensable preliminary step for conducting spectroscopic measurements and performing theoretical calculations for these substances.

5.1.4 Protein crystallography

At the beginning of my scientific career at the Laboratory of Crystalochemistry at the Faculty of Chemistry of the University of Warsaw, in 2003 I had the opportunity to take an 8-month internship in Huntsville, AL, USA. There, I worked on the solution and refinement of the crystal structure of the human dihydrolipoamide dehydrogenase (PDB code: 1ZY8), a fragment of a large enzymatic complex. Solving the protein structure that occurs in more than one copy in an asymmetric unit and shows structural disorder is a challenge even today; this type of problem often results in abandoning the structure solution. The fact that I was able to propose a structural model of the complex, in which the main chain had 474 amino acids and appeared in 10 copies was a significant achievement, documented by the publication [B5].

More recently, I participated in preparing teaching courses on Protein Crystallography, as a part of the undergraduate crystallography course at the Faculty of Chemistry, University of Warsaw.

5.1.5 Ruthenium metathesis catalysts

During my PhD, I performed numerous X-ray structural analyzes for ruthenium-based metathesis catalysts. I took part in the discussion on the relationship between the structure of these catalysts and their catalytic activity, in particular to assess the role of individual ligands in these ruthenium complexes for the efficiency of catalysis at various stages of reaction (solid structure can be related mainly to the catalyst activation stage and initiation of the reaction). The results of my crystallographic analyzes contributed to 7 publications: [B4, B8, B9, B12, B17] [A5, A7]

5.1.6 Other scientific interests

In the course of my scientific career, I performed a number of crystal structure analyzes for a few research groups, which resulted in a few publications. Unless mentioned above, my contributions to these publications consisted of crystal structure determination by means of single-crystal X-ray diffraction and describing the results.

Anna Makal